NOVA SCHOOL OF SCIENCE & TECHNOLOGY

DEPARTMENT OF LIFE SCIENCES

ANDREIA DOS REIS BISPO

BSc in Biochemistry

CHARACTERIZATION OF TWO NEWLY IDENTIFIED *CHLAMYDIA TRACHOMATIS* INCLUSION MEMBRANE PROTEINS

MASTER IN MOLECULAR GENETICS AND BIOMEDICINE

NOVA University Lisbon

September, 2024

NOVA SCHOOL OF SCIENCE & TECHNOLOGY

DEPARTMENT OF LIFE SCIENCES

CHARACTERIZATION OF TWO NEWLY IDENTIFIED *CHLAMYDIA TRACHOMATIS* INCLUSION MEMBRANE PROTEINS

ANDREIA DOS REIS BISPO

BSc in Biochemistry

Adviser: Luís Jaime Gomes Ferreira da Silva Mota,
Associate Professor, NOVA School of Science and Technology

Examination Committee:

Chair: Pedro Manuel Brôa da Costa,
Assistant Professor, NOVA School of Science and Technology

Rapporteurs: Elsa Maria Ribeiro dos Santos Anes,
Full Professor, Faculdade de Farmácia da Universidade de Lisboa

Adviser: Luís Jaime Gomes Ferreira da Silva Mota,
Associate Professor, NOVA School of Science and Technology

MASTER IN MOLECULAR GENETICS AND BIOMEDICINE

NOVA University Lisbon
September, 2024

Characterization of two newly identified *Chlamydia trachomatis* inclusion membrane proteins

ACKNOWLEDGMENTS

First, I would like to thank my advisor, Prof. Jaime Mota, for his support, guidance, patience, encouragement, and for always being present throughout all my Master's journey. His constant availability and support helped me a lot and made this step so much more attainable.

I am also grateful to all my colleagues in the lab and neighbouring research groups, especially Maria, for all her support, availability and kindness. And also, Ana Rita, who started as a colleague and is now a great friend of mine, that was always with me in the lab and shared many laughs, hardships and conversations throughout all this past year. And to Irina, Inês, Lúcia, Eduardo and Bárbara, for all their support and company, especially during lunch. Special thanks to NOVA School of Science and Technology for providing the resources and facilities necessary for this project.

To all my amazing friends, who now know so much more about *Chlamydia*, I am very grateful for having all of you in my life. So, thank you, Bruna, André, Inês, Raquel, Maria, Gonçalo, Pedro e Emma, for all your company and support.

Finally, I am so grateful to my mum, dad, brother and Nino, for their unconditional love, support and patience. Thank you for all your encouragement and for believing in me.

ABSTRACT

Chlamydia trachomatis is a human pathogen that causes genital and ocular infections worldwide. It is an obligate intracellular bacterium that alternates between an infectious (EB, elementary body) and a replicative (RB, reticulate body) form during an infectious cycle in which chlamydiae localizes inside a membrane-bound vacuole known as an inclusion. To manipulate host cell processes from within the inclusion, *C. trachomatis* delivers several effector proteins into the host cell through a type III secretion system. Some of these effectors, known as Incs, possess hydrophobic domains enabling their insertion into the inclusion membrane. Some Incs localize at specific regions of the inclusion membrane, termed microdomains. We previously identified *C. trachomatis* CT195 and CT214 as two putative Incs. To test if they are bona fide Incs, in this work, we first analyzed their subcellular localization in infected cells by immunofluorescence microscopy. This revealed that they localized in the inclusion membrane in all time points assessed, i.e., they are bona fide Incs, and that CT214 also localized in microdomains at the inclusion membrane. Furthermore, we generated and characterized a *C. trachomatis ct195* mutant strain. By comparing cells infected by CT195-producing (parental and complemented strains) or CT195-deficient C. *trachomatis*, we showed that CT195 reduced the chlamydial intracellular growth and delayed the homotypic fusion between inclusions. This suggests that CT195 regulates chlamydial growth; however, the underlying mechanism and relevance of this role of CT195 are presently unknown. We also showed that CT195, like other Incs, contributes to induce multinucleation in infected cells, indicating that it is involved in the known ability of *C. trachomatis* to inhibit host cell cytokinesis. Overall, this work allowed to increase the current knowledge on Incs, a family of important *C. trachomatis* virulence proteins.

Keywords: *Chlamydia trachomatis*; effectors; Inc proteins; membrane microdomains; cytokinesis

RESUMO

Chlamydia trachomatis é uma bactéria patogénica que causa infeções oculares e genitais em todo o mundo. É uma bactéria obrigatoriamente intracelular que transita entre uma forma infeciosa (EB, corpo elementar) e uma replicativa (RB, corpo reticulado), durante um ciclo infecioso, no qual as chlamydiae se localizam dentro de um vacúolo conhecido como inclusão. De forma a conseguir manipular processos da célula hospedeira a partir do interior da inclusão, *C. trachomatis* transporta várias proteínas efetoras para a célula hospedeira através de um sistema de secreção do tipo III. Algumas destas proteínas efetoras, conhecidas como Incs, possuem domínios hidrofóbicos que lhes permitem inserirem-se na membrana da inclusão. Algumas Incs localizam-se em locais específicos da membrana da inclusão, denominados de microdomínios. Anteriormente, identificámos as proteínas CT195 e CT214 da *C. trachomatis* como Incs putativas. Neste trabalho, para testar se CT195 e CT214 eram bona fide Incs, começámos por analisar a sua localização em células infetadas por microscopia de imunofluorescência. Isto revelou que estas proteínas se localizaram na membrana da inclusão em todos os tempos testados, ou seja, que são bona fide Incs. Revelou também que CT214 se localizava em microdomínios na membrana de inclusão. De seguida, construímos e caracterizámos uma estirpe mutante de *C. trachomatis* para o gene *ct195*. Por comparação entre células infetadas por *C. trachomatis* que produzem CT195 (estirpe parental e complementada) ou deficiente em CT195, mostrámos que CT195 reduziu o crescimento intracelular de *C. trachomatis* e atrasou a fusão entre inclusões. Isto sugere que CT195 regula o crescimento de *C. trachomatis*. O mecanismo e relevância deste papel de CT195 são desconhecidos. Adicionalmente, mostrámos que CT195, tal como outras Incs, contribui para promover a multinucleação em células infetadas, indicando que a proteína está envolvida na capacidade conhecida de *C. trachomatis* de inibir a citocinese da célula hospedeira. Em suma, este trabalho permitiu aumentar o conhecimento atual sobre Incs, uma família importante de proteínas de virulência de *C. trachomatis*.

Palavras chave: *Chlamydia trachomatis*; proteínas efetoras; proteínas Inc; microdomínios membranares; citocinese

CONTENTS

LIST OF FIGURES

List of Tables

ABBREVIATIONS

Amp	Ampicillin
aRB	aberrant Reticulate body
ATCC	American Type Culture Collection
BACTH	Bacterial Adenylate Cyclase-based Two-Hybrid
bp	base pairs
cAMP	cyclic Adenosine Monophosphate
CRISPRi	Clustered Regularly Interspaced Short Palindromic Repeats interference
CT-FITC	Chlamydia trachomatis-Fluorescein Isothiocyanate
DAPI	4',6-diamidino-2-phenylindole
DMEM	Dulbecco's Modified Eagle Medium
DNA	Deoxyribonucleic Acid
EB	Elementar Body
ECACC	European Collection Authenticated of Cell Cultures
ER	Endoplasmic Reticulum
FBS	Foetal Bovine Serum
Fw	Forward
HA	Hemagglutinin
HBSS	Hank's Balanced Salt Solution
His-tag	Polyhistidine-tag
HPV	Human Papillomavirus
IEP	Intron-Encoded Protein
IFU	Inclusion Forming Units
Inc protein	Inclusion membrane protein
IPTG	Isopropyl β-D-1-thiogalactopyranoside
Kan	Kanamycin
LB	Lysogeny Broth
LGV	Lymphogranuloma Venereum

MCS	Membrane Contact Sites
MOI	Multiplicity Of Infection
MOMP	Major Outer Membrane Protein
mRNA	messenger Ribonucleic Acid
NEB	New England Biolabs
OD	Optical Density
p.i.	post-infection
PAMAM	Poly(amidoamine)
PBS	Phosphate Buffered Saline
PCR	Polymerase Chain Reaction
PFA	Paraformaldehyde
RB	Reticulate Body
RNA	Ribonucleic Acid
rpm	rotation per minute
Rv	Reverse
SDS-PAGE	Sodium Dodecyl Sulfate-Polyacrylamide Gel Electrophoresis
SEM	Standard Error of the Mean
SPG	Sucrose Phosphate Glutamate
Spm	Spectinomycin
T2SS	Type II Secretion System
T3SS	Type III Secretion System
UI	Uninfected
X-Gal	5-bromo-4-cloro-3-indoxil-β-D-galactopiranosídeo

1

INTRODUCTION

1.1 *Chlamydia trachomatis*

Chlamydia trachomatis is a gram-negative obligate intracellular bacterium. It is a human pathogen that is the cause of most sexually transmitted infections, and it is the leading cause of infection-related blindness around the world (Mohseni et al., 2023). In 2020, there were approximately 129 million of new genital infections globally caused by *C. trachomatis* (World Health Organization, 2023). These genital infections are mostly transmitted by intercourse, but transmission can also occur from mother to a newborn baby during delivery (Mohseni et al., 2023). The infections can easily be diagnosed by PCR and treated with antibiotics, and most of the cases are asymptomatic (70% in women and 50% in men) (European Centre for Disease Prevention and Control, 2017). If not treated, they can lead to infertility and blindness, in case of genital and ocular infections, respectively.

C. trachomatis has 15 main serovars. The differences between each one of them is based on the antigenic variance of its major outer membrane protein (MOMP). Each serovar belongs to one of three biovars: the trachoma biovar (serovars A-C), the genital biovar (serovars D-K) and the lymphogranuloma venereum (LGV) biovar (serovars L1-L3). Even though the genital strains are the cause of the most infections (Nunes & Gomes, 2014), research on the interactions between the host cell and the chlamydiae is usually done using a prototype serovar L2 strain as model (Bugalhão & Mota, 2019).

Infection by both *C. trachomatis* and human papillomavirus (HPV) induce amplification of centrosomes, which is a characteristic feature of cancer cells. When cells are infected with both pathogens, although they induce this amplification by different mechanisms, their effects are additive. *Chlamydia* has a greater effect as it leads to a failure in cytokinesis, resulting in multinucleation. This further suggests that *C. trachomatis* could as a cofactor for HPV in carcinogenesis in a co-infection situation (Wang et al., 2021; Zhu et al., 2016).

1.2 *C. trachomatis* developmental cycle

C. trachomatis belongs to the *Chlamydiales* order and all organisms of this order share the particularity of developing in a cycle involving two distinct morphological forms, the infectious and non-replicative elementary bodies (EBs; ~ 0.3 µm in diameter in *C. trachomatis*) and the replicative but non-infectious reticulate bodies (RBs; ~ 1 µm in diameter in *C. trachomatis*), that differentiate one into other during the cycle. In *C. trachomatis*, the cycle can last 48 to 72 h, depending on the strain. This cycle involves the formation of a nonacidified vacuole that is referred as inclusion and is needed so the bacteria can grow within eukaryotic cells (Bugalhão & Mota, 2019).

The cycle starts with the attachment of EBs to the surface of the host cell (Figure 1.1), this interaction triggers the release of chlamydial effector proteins through one of *Chlamydia* secretion systems, the type III secretion (T3S) system. These effectors mediate actin rearrangements allowing the internalization of EBs through the host cell membrane thus forming the inclusion. They also ensure the bacterial survival in the host cell by preventing its interaction with endocytic pathways and by influencing host cell survival and immune signalling. The entrance of EBs in host cell marks the beginning of infection (0 h of infection). After 2 h, EBs start to differentiate into RBs and by 6 h post infection (p.i.), RB replication initiates. Simultaneously, the inclusion migrates along microtubules toward the perinuclear (around the nucleus) and centrosomal regions. Due to the increase of the RB population, the inclusion expands to the point of occupying most of the host cell's cytosol (Bugalhão & Mota, 2019).

Under adverse conditions such as the exposure to antibiotics, cytokines or nutrient deprivation, *C. trachomatis* can enter a reversible persistent state, forming aberrant reticulate bodies (aRBs) (Figure 1.1). To ensure its survival, aRBs adapt their metabolism and gene expression differently depending on the trigger to conserve energy and resources. This results in stopping their division thus leading to a larger size and a halt in the production of infectious particles. This state is easily reversible once the inducer is no longer present (Panzetta et al., 2018; Kozusnik et al., 2024).

Beginning at 24h p.i. and until the end of the cycle, it occurs the desynchronized re-differentiation of RBs into EBs. The inclusion becomes filled with EBs, which are capable of infecting the neighbouring cells after their release. These EBs are known as the infectious progeny. Their release can occur either through host cell lysis or by extrusion (Figure 1.1) (Bugalhão & Mota, 2019).

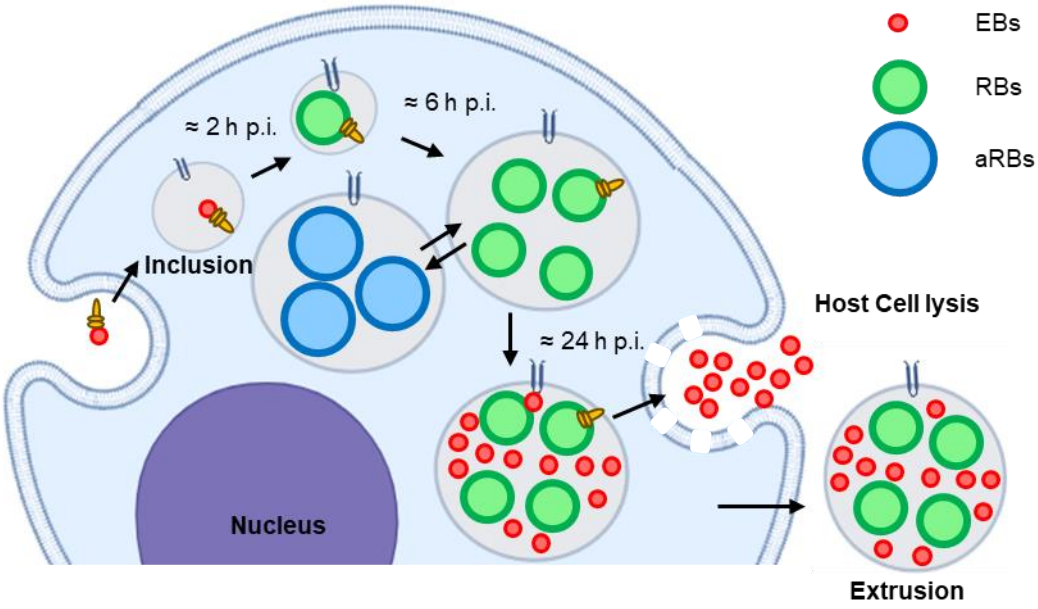

Figure 1.1. Chlamydia developmental cycle. The cycle involves three forms, elementary bodies (EBs), reticulate bodies (RBs) and aberrant RBs (aRBs). It starts with the adhesion of EBs to the host cell's membrane that leads to the formation of a membrane bound vacuole, known as the inclusion. EBs then differentiate into RBs and when it an appropriate intracellular environment is establishing, RBs begin to replicate. Later, RBs start to re-differentiate into EBs that are released to extracellular space by extrusion or lysis. aRBs are formed when the bacteria are subjected to exposure to adverse conditions, such as antibiotics or interferons. Created with BioRender.com

1.3 Development of genetic manipulation of *C. trachomatis*

The characteristics of being an obligate intracellular pathogen with a unique developmental cycle have posed major challenges in the genetic manipulation of *C. trachomatis*. For years, knowledge about the function of its proteins has faced limitations due to the lack of effective genetic tools.

It is challenging for exogenous DNA to reach the bacterial cytoplasm in the form of RB, which is exclusively found inside of the inclusion within host cell, thus having to penetrate several membranes layers. In the case EBs, that can be found and survive outside of the host cell, their rigid cell wall and low metabolic activity makes it difficult to absorb and integrate external DNA (Wan et al., 2023).

In recent years, there has been enormous progress in developing genetic tools to manipulate *C. trachomatis*. The usual first step in these methods is the transformation of *Chlamydia*. Four methods have been initially developed: electroporation, chemical mutagenesis, polyamidoamine dendrimer (PAMAM dendrimers) and $CaCl_2$ transformation (Wan et al., 2023), but these days $CaCl_2$ transformation is the standard procedure.

Electroporation can be used in obligate intracellular bacteria to effectively introduce foreign DNA by inducing cell membrane permeabilization through electric pulses. This permeabilization is transient and reversible (Tam et al., 1994). Although the method is efficient, fast and allows gene expression from foreign DNA, it also has its limitations. It requires highly purified EBs, the use of heterologous screening tags, and part of the bacteria is damaged. Due to its limitations, it has not been widely adopted.

Chemical mutagenesis has been used to mutate *C. trachomatis* DNA by exposing it to alkylating agents (chemical mutagens). Depending on the concentration of the mutagen, it is possible to obtain one or multiple mutations per genome. (Kokes et al., 2015) This method is a fast, simple and non-expensive that allows direct mutation of the bacteria in host cells. However, it is a laborious and tedious process, and as a result of only allowing to generate random mutants, most of the obtained mutants are from non-essential genes.

PAMAM dendrimers are polymers, that with their low cytotoxicity are capable of delivering small molecules to specific sites and transfer macromolecules like plasmid DNA and oligonucleotides into cells. In the case of *Chlamydia*, these polymers have been efficiently used to transform RBs in infected cells, by transferring plasmids but also antisense oligonucleotides to knockdown a specific gene (Manoj Kumar Mishra et al., 2012; Kannan et al., 2013). Although having all this advantages, it is an expensive method, which is probably the reason for not being widely used.

$CaCl_2$ transformation consist in a first incubation of EBs with the endogenous DNA in $CaCl_2$ buffer followed by an incubation with host cells in the same buffer (Wang et al., 2011). Its limits are the low efficiency in transformation and the need of an antibiotic selection. However, it remains widely used to its speed, simplicity, low cost, and ease of operation. Due to this, $CaCl_2$ transformation is widely used to transform *Chlamydia*. This method serves as a way to integrate the exogenous DNA, so to generate mutants other approaches are needed. Some methods often used in association with the $CaCl_2$ transformation, include the group II intron-based targeted gene knockout, CRISPR interference (CRISPRi) and transposon insertion mutagenesis.

For example, group II introns are self-splicing ribozymes that can move between genes by a process named retrohoming, in which the intron RNA reverse splices into a specific DNA site, followed by reverse transcription by intron-encoded protein (IEP) (Key & Fisher, 2016). Based on this principle, the TargeTron system has been developed, which allows the knockout of the target gene by the insertion of a group II intron with antibiotic selective marker. This method was used in this work to knockout the target genes. To determine the insertion site, it is necessary bioinformatic analysis to design several insertion sites to guarantee likelihood of a successful knockout. This method is costly and like all gene insertion methods has the possibility of polar effects on the expression of neighbouring genes if the knockout gene exist within polycistronic operons (Wan et al., 2023).

Most of the *C. trachomatis* mutants obtained to date, were obtained by using group II intron-based targeted gene knockout (O'Neill et al., 2020). In this work, it was used this method to obtain the mutant of the target genes.

1.4 Type III Secretion System (T3SS)

As a Gram-negative bacterium, *C. trachomatis* uses several protein transport systems like the Sec system, a type II secretion system (T2SS), and a type III secretion system (T3SS) (Bugalhão & Mota,

2019). T3SS is one of the most important, allowing interaction with the host cell by injecting effector proteins directly into it (Figure 1.2). However, some T3SS substrates have also been found at the inclusion lumen (da Cunha et al., 2017).

These effector proteins have roles in manipulating host cell processes and evading immune responses. Thus, this system allows *C. trachomatis* to control host cell functions to its benefit, ensuring its invasion and intracellular survival. The most prominent group of T3SS effectors are the inclusion membrane proteins (Incs), which, after translocation, are inserted into the inclusion membrane (Figure 1.2) (Elwell et al., 2016).

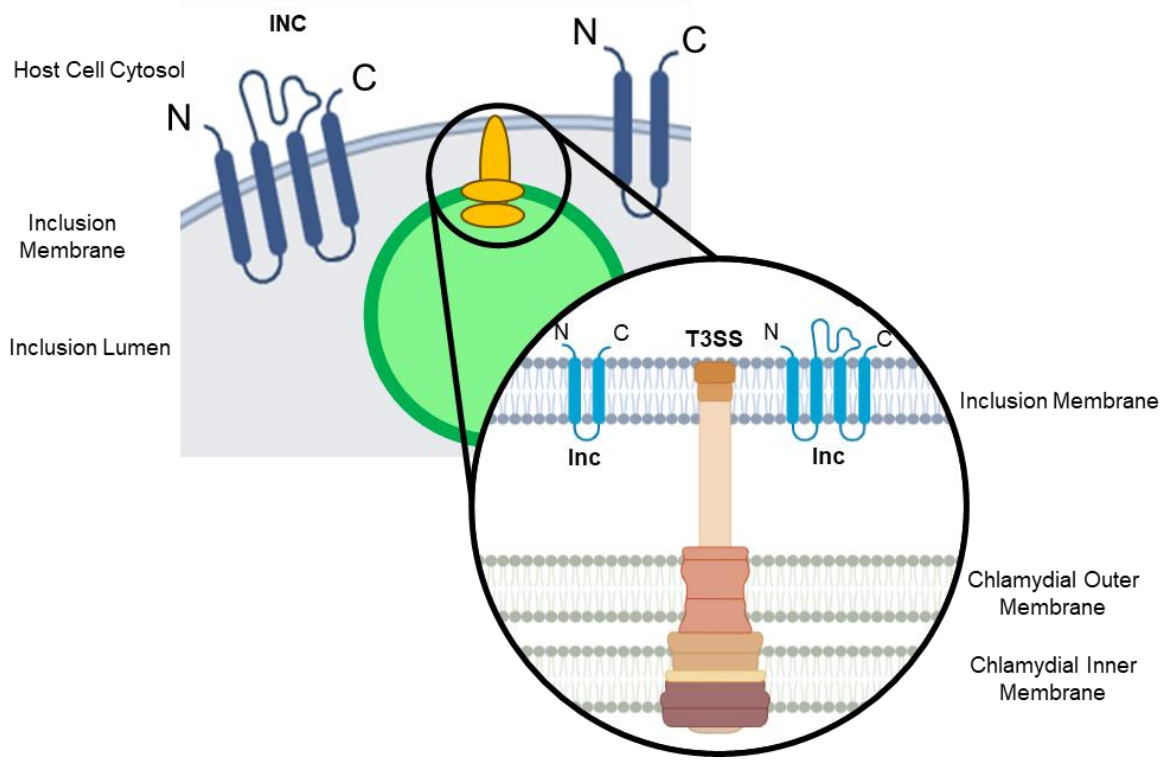

Figure 1.2. Predicted chlamydial Type III Secretion System. This system is present in Gram-negative bacteria and allows the transport of effectors from the bacterial cytoplasm into the host cell cytosol. Created with BioRender.com. Inc – inclusion membrane protein.

1.5 Inclusion membrane proteins (Incs)

Incs are characterized by their localization at the inclusion membrane and for exhibiting one or more bilobed hydrophobic domains, which is a determinant of their localization (Figure 1.3). The hydrophobic domain consists of 40-60 residues, containing two transmembrane α-helices that allow the insertion of these proteins into the inclusion membrane, separated by a loop of less than 30 hydrophilic residues. It is predicted that at least one end extends into the host cell's cytoplasm (Elwell et al., 2016). However, the presence of this domain in Incs does not guarantee translocation to the inclusion membrane (Dehoux et al., 2011).

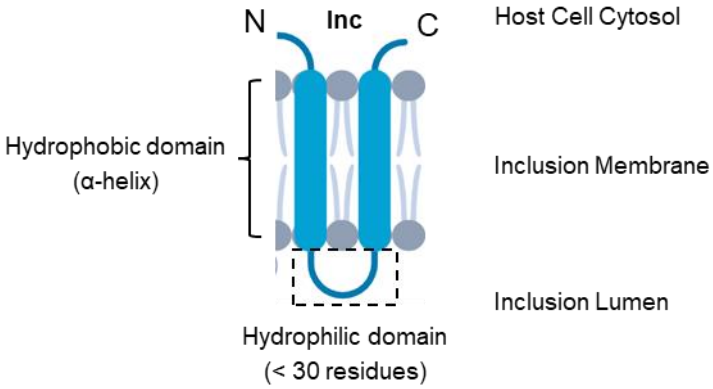

Figure 1.3. Inclusion membrane proteins (Incs). Incs have at least one bilobed hydrophobic domain, which includes two α-helices that allows the insertion of the protein in the inclusion membrane and are separated by a hydrophilic domain of less than 30 residues.

From the analysis of the *C. trachomatis* genome, 59 putative Incs have been predicted by computational methods based on the presence of bilobal hydrophobic domains (Weber et al., 2015). Some studies have identified 36 of these proteins as bona fide Incs because of their localization at the inclusion membrane (Table 1.1; Bugalhão & Mota, 2019). Most of these identifications occur through the generation of fusion proteins of Incs with epitope tags (Weber et al., 2015) or by generating anti-Inc antibodies (Li et al., 2008). In a 2015 study, aimed to determine the localization of bioinformatically predicted Incs, two putative Incs found associated with the bacteria (CT195 and CT365) were identified as T3SS substrates (Weber et al., 2015).

Table 1.1. Predicted Incs

Predicted Incs			Localization
General	**D/UW-3/CX**	**L2/434/Bu**	
IncV	CT005	CTL0260	Inclusion membrane[1,2]
	CT006	CTL0261	Inclusion membrane[2]
	CT036	CTL0291	Bacteria[2]
	CT058	CTL0314	Intrainclusion[2]
	CT079	CTL0335	Bacteria[2]
	CT089	CTL0344	Inclusion membrane[2]
MrcA	CT101	CTL0356	Inclusion membrane[3]
IncD	CT115	CTL0370	Inclusion membrane[2]
IncE	CT116	CTL0371	Inclusion membrane[2]
IncF	CT117	CTL0372	Inclusion membrane[2]
IncG	CT118	CTL0373	Inclusion membrane[2]
IncA	CT119	CTL0374	Inclusion membrane[2]
	CT134	CTL0389	Inclusion membrane[2]
GarD	CT135	CTL0390	Inclusion membrane[2]

[1] Not explained how they detected (Shaw et al., 2000)
[2] Obtained by cloning genes with Tet or Tac promoter (Li et al., 2008; Weber et al., 2015)
[3] Detected by using antibodies that specifically bind to the protein (Belland et al., 2003; Mital et al., 2010b)

	CT147	CTL0402	Inclusion membrane[3]
	CT164	CTL0419A	Not defined[2]
	CT179	CTL0431	Inclusion membrane[2]
Dre1	CT192	CTL0444	Inclusion membrane[2]
	CT195	CTL0447	Bacteria[2]
	CT196	CTL0448	Not defined[2]
	CT214	CTL0466	Bacteria[2]
	CT222	CTL0475	Inclusion membrane[3]
IPAM	CT223	CTL0476	Inclusion membrane[2]
Tri1	CT224	CTL0477	Inclusion membrane[2]
	CT225	CTL0477A	Inclusion membrane[2]
	CT226	CTL0478	Inclusion membrane[2]
	CT227	CTL0479	Inclusion membrane[2]
	CT228	CTL0480	Inclusion membrane[2]
CpoS	CT229	CTL0481	Inclusion membrane[2]
IncB	CT232	CTL0484	Inclusion membrane[2]
IncC	CT233	CTL0485	Inclusion membrane[2]
	CT244	CTL0496	Bacteria[2]
	CT249	CTL0500A	Inclusion membrane[2]
IncM	CT288	CTL0540	Inclusion membrane[2]
	CT300	CTL0552	Not defined[2]
	CT324	CTL0576	Not defined[2]
	CT345	CTL0599	Inclusion membrane[2]
	CT357	CTL0611A	Not defined[2]
	CT358	CTL0612	Inclusion membrane[2]
	CT365	CTL0619	Bacteria[2]
	CT383	CTL0639	Inclusion membrane[2]
	CT440	CTL0699	Inclusion membrane[2]
CrpA	CT442	CTL0701	Inclusion membrane[2]
	CT449	CTL0709	Inclusion membrane[2]
	CT483	CTL0744	Inclusion membrane[1]
	CT484	CTL0745	Intrainclusion[2]
	CT529	CTL0791	Inclusion membrane[2]
	CT565	CTL0828	Inclusion membrane[1]
	CT616	CTL0880	Bacteria[2]
	CT618	CTL0882	Inclusion membrane[2]
	CT642	CTL0010	Bacteria[2]
	CT728	CTL0097	Bacteria[2]
	CT788	CTL0156	Bacteria[2]
	CT789	CTL0157	Bacteria[2]
InaC	CT813	CTL0184	Inclusion membrane[2]
	CT819	CTL0191	Bacteria[2]
	CT846	CTL0218	Bacteria[2]
	CT850	CTL0223	Inclusion membrane[3]

The messenger RNA (mRNA) levels of *inc* gene can be higher at certain stages of the chlamydial developmental cycle (Shaw et al., 2000) Therefore, Incs have been divided into 3 classes according to the stage of the cycle at which their levels are the highest: early-cycle (2-6 h p.i.), mid-cycle (6-20 h p.i.) or late-cycle (>20 h p.i.) (Bugalhão & Mota, 2019; Shaw et al., 2000).

Some of the Incs (MrcA, CT222, IPAM, CT224, CT228, IncB, IncC, IncM and CT850) also localize in specific regions at the inclusion membrane, named microdomains (Weber et al., 2015; Lutter et al., 2013; Mital et al., 2010). These microdomains has been observed in some cases to localize near the centrosome and it is thought that they mediate interactions with the centrosome, actin cytoskeleton and microtubules (Mital et al., 2010).

Although they share the localization at the inclusion membrane, there is a great diversity of functions among Incs. They have been shown to contribute to several abilities of *Chlamydia* (Table 1.2), as described next.

Table 1.2. Proposed function of *C. trachomatis* Incs

Proposed function		Inc[4]	References
Host cell vesicular and nonvesicular trafficking	ER-inclusion MCS and nonvesicular lipid uptake	IncV	(Stanhope et al., 2017; Wenbo et al., 2024)
		IncD	(Derré et al., 2011; Wenbo et al., 2024)
	Host vesicular trafficking	IncE	(Elwell et al., 2017; Wenbo et al., 2024)
		IncA	(Cingolani et al., 2019; Wenbo et al., 2024)
		CpoS	(Faris et al., 2019; Wenbo et al., 2024)
Inclusion fusion		IncA	(Hackstadt et al., 1999)
Microtubule network		IPAM	(Dumoux et al., 2015)
		InaC	(Haines et al., 2021; Wesolowski et al., 2017)
Inclusion migration		CT850	(Mital et al., 2015)
Distribution of Golgi		Dre1	(Sherry et al., 2022)
		IncM	(Luís et al., 2023)
		InaC	(Wesolowski et al., 2017)
Positioning of centrosome		Dre1	(Sherry et al., n.d.)
		IncM	(Luís et al., 2023)
		CT850	(Mital et al., 2010a)
Inhibit cytokinesis		IPAM	(Alzhanov et al., 2009)
		Tri1	
		CT225	
		Dre1	(Sherry et al., 2022)
		IncM	(Luís et al., 2023)

[4] Specific names used to these Incs; CT000 refers to the D/UW3 strain nomenclature

Select release process		MrcA	(Nguyen et al., 2018)
		GarD	(Bishop & Derré, 2022)
		CT228	(Lutter et al., 2013)
Evade Host Immune Response	Prevents host cell death	IncE	(Wang et al., 2024)
		IncG	(Verbeke et al., 2006)
		IncA	(Ronzone & Paumet, 2013)
		GarD	(Walsh et al., 2022)
		CpoS	(Sixt et al., 2017)
	Controls Inclusion membrane stability	CpoS	(Weber et al., 2017)
		IncC	
		IncM	(Luís et al., 2023)
		CT383	(Weber et al., 2017)
		InaC	

Through the action of Incs, *C. trachomatis* modulates host cell vesicular and nonvesicular trafficking to evade phagolysosomal pathway and to obtain nutrients, mediates homotypic fusion, a process in which inclusions fuse with each other, inhibits cytokinesis leading to host cell multinucleation, selects its release process (extrusion or lysis), evades host immune response by preventing host cell death and controlling inclusion membrane stability (Bugalhão & Mota, 2019). Incs also help *C. trachomatis* to modulate microtubules to allow inclusion migration, distribute the fragmented Golgi complex (Heuer et al., 2008) and alter the positioning of the centrosome.

In addition to interacting with host cell proteins, Incs also interact with each other, possibly to increase their efficiency in manipulating the host cell, and maintaining the integrity of the inclusion membrane. For example, homotypic IncA:IncA interactions mediate homotypic fusion. Among Incs, some have a larger portion of their polypeptide chains predicted to be oriented toward the host cell's cytosol, compared to others that may have less than 30 residues. This might imply that those with smaller regions may be mainly involved in interactions with others Incs (Bugalhão & Mota, 2019). Several Inc proteins have been found to participate in homo-oligomerization (IncD, CT223, CT222, IncF, CT249, IncA, IncC, CT005, CT225 and CT813) and heterophilic Inc:Inc interactions (CT005, CT058, IncD, IncF, IncG, IncA, CT222, CT229, CT249, CT233 and CT850) (Figure 1.4). In the case of IncA, both its transmembrane and cytoplasmic domains contribute independently to its oligomerization. For CT222, it has been reported that its transmembrane domain is responsible for both its oligomerization and interaction with CT850 (Gauliard et al., 2015).

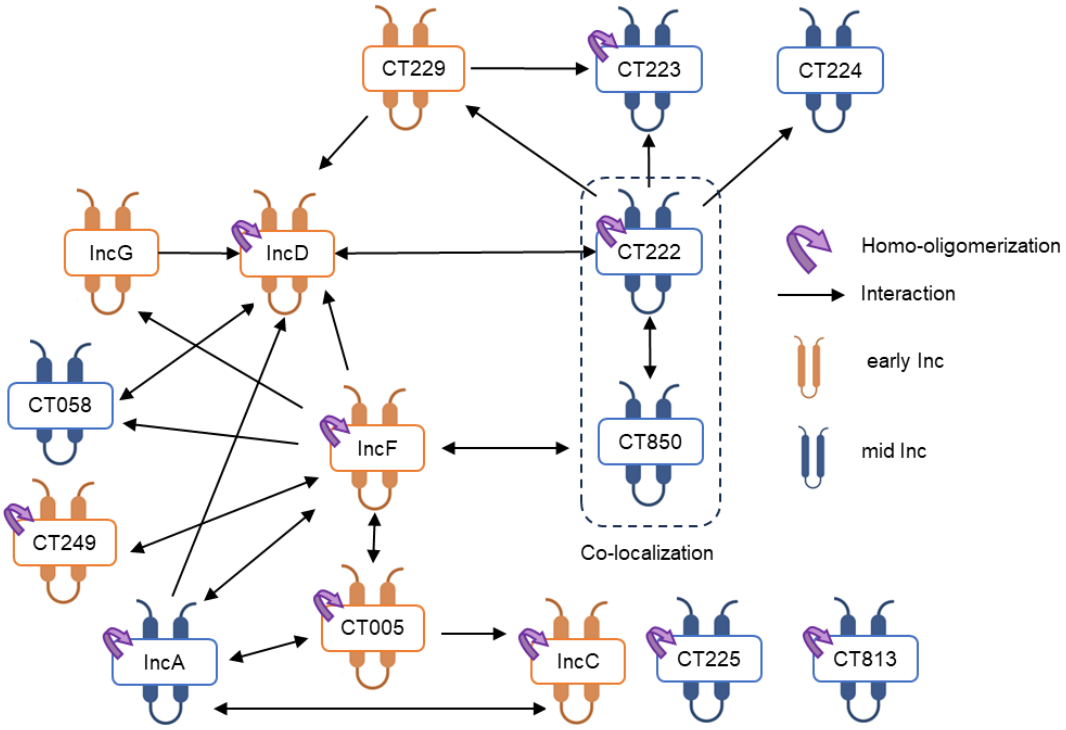

Figure 1.4. Interactions between inclusion membrane proteins. Adapted from Gauliard et al., 2015. Inc – inclusion membrane proteins.

1.6 Aims

Unpublished studies with *C. trachomatis* IncM revealed that its timing of secretion and precise localization at the inclusion membrane varies according to whether the encoding gene is expressed from its own promoter, from the promoter of another *inc* gene (*incD*) or from tetracyline promoter (Maria Pequito Luís and Luís Jaime Mota, unpublished). This led us to screen if putative Incs previously found to localize inside the inclusion after expression from the tetracyline promoter (Weber et al., 2015) could localize at the inclusion membrane when produced after expression from their own promoters. This led to the identification of CT195 and CT214 as two novel putative bona fide Incs (Maria Pequito Luís and Luís Jaime Mota, unpublished).

In this work, to further the understanding on how *C. trachomatis* manipulates host cells through Incs, we aimed to:

- Determine if CT195 and CT214 are bona fide Incs by characterizing their localization at the inclusion membrane.
- Generate *C. trachomatis* mutants deficient for CT195 and/or CT214.
- Obtain insights on the function of CT195 and/or CT214 through the characterization of the mutant strains.

2

MATERIALS AND METHODS

2.1 Mammalian cell lines

HeLa and Vero cells (all from the European Collection Authenticated of Cell Cultures; ECACC) were routinely maintained in DMEM (high-glucose Dulbecco's modified Eagle Medium; Corning) supplemented with 10% (v/v) FBS (heat-inactivated foetal bovine serum; Thermo Fisher Scientific) at 37°C in a humidified atmosphere of 5% (v/v) CO_2.

2.2 Bacterial strains and growth conditions

The bacterial strains used in this work are described in Table A. 1 and Table A. 2, in Annexes. *E. coli* NEB® 10β (New England Biolabs) was used for the construction and purification of all plasmids, *E. coli* BTH101 (Dautin et al., 2000) was used in the bacterial two-hybrid assay, and the methylation-deficient *E. coli* ER2925 (New England Biolabs) was used to amplify and purify plasmids for the transformation of *C. trachomatis*. These strains were grown at 37°C in liquid or solid LB (lysogeny broth) medium with the appropriate antibiotics. Plasmids were introduced into these strains by electroporation or by heat shock of calcium-competent *E. coli* cells.

The *C. trachomatis* LGV serovar L2 strain 434/BU (L2/434; from the American Type Culture Collection, ATCC) was cultured in HeLa 229 cells following conventional methods (Scidmore, 2005). The nomenclature of the annotated *C. trachomatis* D/UW3 strain (Stephens et al., 1998) was used throughout this work.

2.3 Preparation of *E. coli* competent cells

For electrocompetent or calcium-competent *E. coli* cells, an isolated colony was inoculated in 5 mL of LB with appropriate antibiotics and grown overnight at 37°C, 150 rpm. A 1:100 dilution of the overnight culture was made (final volume of 300 mL of LB for electrocompetent cells and 50 mL of LB

for chemically competent cells) and the bacterial culture was incubated under the same conditions until an optical density at 600 nm (OD_{600}) of 0.5 was reached. Then, the cells were divided into tubes and kept on ice for 30 min.

Electrocompetent cells were obtained by four centrifugations at 5,000 rpm, for 10 min, 4°C. After each centrifugation, the pellet was resuspended in ice-cold bid-H_2O for the first two centrifugations (300 and 150 mL, respectively) and in ice-cold 10%(v/v) glycerol for the remaining centrifugations (50 and 1.5 mL, respectively).

To obtain chemically competent cells, three centrifugations were performed at 4,000 rpm, for 10 min, 4°C. After each centrifugation, the pellet was resuspended in 5 mL of ice-cold $MgCl_2$ 0.1 M, for the first one, and ice-cold $CaCl_2$ 0.1M for the remaining centrifugations (5 and 1.6 mL, respectively). After all centrifugations, 200 µL of ice-cold sterile 50% (v/v) glycerol was added to the cells in ice-cold $CaCl_2$ 0.1M.

2.4 Plasmids, primers, and DNA manipulation

The plasmids and DNA primers utilized in this work, as well as their main characteristics, are presented in Table A. 3 and Table A. 4, respectively, in Annexes. The backbone plasmids utilized in this study include pDFTT3aadA (Key and Fisher, 2016), pUT18C, and His-pKT25, which pDFTT3aadA was used in the generation of the *ct195* and *ct214*-group II intron donor plasmid, while pUT18C and His-pKT25 were used to construct the interest plasmids for the bacterial two-hybrid assay. DNA sequencing was used to verify the accuracy of the nucleotide sequence of the constructed plasmids.

All the plasmids generated during this work were obtained utilizing standard molecular biology procedures Phusion™ high-fidelity DNA polymerase, restriction enzymes, T4 DNA Ligase (all from Thermo Fisher Scientific) and kits such as DNA clean and concentrator™-5, Zymoclean™ gel DNA recovery (Zymo Research), and NZYMiniprep or NZYMidiprep (NZYtech), were all utilized in accordance with the manufacturers' guidelines. To confirm the presence and size of the plasmids and inserts at several steps of the procedure, PCR was performed using NZYTaq II DNA polymerase (NZYtech).

2.5 Immunofluorescence microscopy

For immunofluorescence microscopy, cells were fixed with methanol for 7 min at -20°C or with 4% (w/v) paraformaldehyde (PFA) for 15 min at room temperature. The cells were then washed with phosphate buffered saline (PBS). Both primary and secondary antibodies were diluted in PBS and 10% (v/v) of horse serum. Then, the coverslips with the cells were washed in PBS and were subjected to a 1 h incubation with primary antibodies. The cells were then washed with PBS and incubated for another hour with secondary antibodies. After this incubation, the cells were washed with PBS and then with

H_2O. The coverslips were then ready to be mounted onto glass slides using Aqua Poly/Mount mounting medium (Polysciences). This procedure was used for cells fixed with methanol. When cells were fixed with 4% (w/v) PFA, the washes were done with PBS with 0.1% (v/v) Triton-X100 instead of PBS. Samples were analysed using a widefield fluorescence microscope (Zeiss AxioImager D2) and images were processed using Fiji.

2.6 Construction of the *C. trachomatis ct195::aadA* and *ct214::aadA* mutant strain

To obtain *C. trachomatis* mutants, it was used the group II intron-based insertional mutagenesis (Key and Fisher, 2016), as previous explained. The intron was retargeted for the genes of interest (*ct195* and *ct214*) by PCR and the resulting DNA product was digested with HindIII and Bsp1407I. The vector pDFTT3aadA was digested with the same enzymes. Then, inserts and vector were both ligated using T4 DNA Ligase, resulting in plasmids pAB1 and pAB2 which potentially allow obtaining *C. trachomatis ct195* and *ct214* mutants. For that, methylation-deficient *E. coli* ER2925 (New England Biolabs) electrocompetent cells were transformed with pAB1 or pAB2 allowing to obtain plasmid DNA that can be used to generate *C. trachomatis* mutants (*ct195::aadA* and *ct214::aadA*). The plasmids generated were used to transform *C. trachomatis* L2/434, as described further below in the *C. trachomatis* transformation section.

2.7 *C. trachomatis* transformation

C. trachomatis L2/434 or *ct195::aadA* were transformed with plasmids pAB1 and pAB2 or pML39 (Table A. 3) as complementation plasmid of CT195, respectively. Initially, 6 µg of plasmid DNA was mixed with 200 µL of $CaCl_2$ buffer (10 mM Tris, 50 mM $CaCl_2$, pH 7,4) by vortexing. Then, 20 µl of L2/434 ($1x10^9$ IFU/ml) stored in SPG (sucrose phosphate glutamate buffer; 0.2 mM sucrose, 17 mM Na_2HPO_4, 3 mM NaH_2PO_4, 5 mM L-glutamic acid) were added homogenized by pipetting up and down, and incubated for 30 min at room temperature. Meanwhile, the pellet of 3×10^6 trypsinized HeLa cells was prepared, by washing the cells with PBS followed by resuspension in 200 µl of $CaCl_2$ buffer. After incubation, the *Chlamydia*/DNA mix in $CaCl_2$ buffer was added to the HeLa cells resuspended in $CaCl_2$ buffer and incubated for 20 min at room temperature with gentle mixing by pipetting up and down every 5 min. This mixture was divided into 2 wells of a 6-well plate each containing 3 ml of DMEM with 10% (v/v) FBS, and then incubated at 37°C in the presence of 5% (v/v) CO_2. After 16 h of incubation, the medium was replaced by fresh DMEM with 10% (v/v) FBS supplemented with the selective antibiotic (0.3 U/ml of penicillin G [Sigma] or 250 µg/ml of spectinomycin). After 48 h, the cells were osmotically lysed by adding 500 µl of sterile dH_2O and incubated for 15 min. Then, 500 µl of double-concentrated SPG (SPG 2x) was added to the lysed cells followed by a 5 min centrifugation at 270 x g, at room temperature. The supernatant was added to previously seeded HeLa cells ($4x10^6$ cells in a 25 cm^2 surface area flask),

washed with Hank's balanced salt solution (HBSS; Invitrogen). The cells with added supernatant containing infectious chlamydiae were incubated 1 h at room temperature, with gentle agitation. After incubation, the inoculum was removed, and DMEM with 10% (v/v) FBS, and the appropriate selective antibiotic was added. This procedure was repeated two or three times under the same conditions. Once inclusions were observed by phase-contrast microscopy, a few more passages were done until many normal inclusions were observed. The aliquots of the transformed chlamydia*e* were maintained at -80°C.

2.8 Clonal Isolation by plaque assay

Initially, $4x10^5$ of Vero cells were seeded into each well of a 6-well plate and incubated at 37°C in the presence of 5% (v/v) CO_2 for 24 h. An aliquot of a transformed *C. trachomatis* strain was thawed and six 10-fold serial dilutions in SPG were done in a total volume of 1.5 ml. Then, 500 µl of each dilution were added to each well of the 6-well plate seeded with Vero cells, previously rinsed with HBSS, and incubated for 30 min at 37°C in a humidified atmosphere with 5% (v/v) CO_2. After that, the inoculum was removed, and DMEM with 10% (v/v) FBS, 1 µg/ml cycloheximide, and the appropriate antibiotic (1U/ml Penincilin G or 250 µg/ml of spectinomycin) was added followed by incubation at 37°C in a humidified atmosphere of 5% (v/v) CO_2 for 24 h. The next day, the medium was removed, and 2 ml of agarose overlay media (6 ml of 1.2% [w/v] melted sterile agarose and 6 ml of DMEM 2x with 10% (v/v) FBS and 1 U/ml Penincilin G or 250 µg/ml of spectinomycin) was quickly added, and left to solidify during 5 min outside of the biosafety hood. Then, 2 ml of liquid overlay media (DMEM [without phenol red] and 10% (v/v) FBS) was added on top of the solid agarose media, and the cells were incubated during 3 or 4 days at 37°C in a humidified atmosphere of 5% (v/v) CO_2, until isolated plaques could be observed. The plaques were then marked, and the agarose removed using a sterile 200 µl barrier pipette tip and resuspended in 100 µl of DMEM with 10% (v/v) FBS, 1 µg/ml cycloheximide and 1U/ml Penicillin G or 250 µg/ml of spectinomycin. On the previous day, Vero cells were seeded in a 96-well plate at $1x10^4$ cells/well to which the 100 µl of the chlamydiae suspension was added. The plates were spun at 2250 x g for 30 min at 15°C and then incubated at 37°C in a humidified atmosphere of 5% (v/v) CO_2. Two days later, the cells were lysed as previously described to collect the *C. trachomatis* strain, which was then stored at -80°C. The procedure was repeated to amplify the desired clone and obtain *C. trachomatis* stocks.

2.9 Antibodies and fluorescent dyes

For immunoblotting, the following antibodies were used at 1:1,000: mouse anti-α-tubulin (Sigma-Aldrich), rat anti-HA 3F10 (Roche), and mouse anti-Hsp60 (Thermo Fisher Scientific). The secondary antibodies horseradish peroxidase-conjugated secondary antibody anti-mouse (GE Healthcare) and anti-rat (Sigma-Aldrich) were used at 1:10,000.

For immunofluorescence, the antibodies used were: rat anti-HA 3F10 (1:200; Roche), goat anti-MOMP (*C. trachomatis* major outer membrane protein; 1:200; Abcam), mouse anti-γ-tubulin (1:200; Sigma-Aldrich), rabbit anti-GM130 (1:200; Sigma-Aldrich), anti-CT-FITC (anti-*C. trachomatis* fluorescein isothiocyanate; 1:100; Milipore), and rabbit anti-IncM (1:10; Almeida et al., 2018). The secondary antibodies (anti-rat conjugated to rhodamine RedX (Jackson ImmunoResearch Laboratories), goat anti-rat AF488 (Jackson ImmunoResearch Laboratories), donkey anti-goat AF488 (Thermo Fisher Scientific), donkey anti-goat AF405 ((Jackson ImmunoResearch), goat anti-mouse AF568 (Invitrogen), anti-rabbit conjugated to rhodamine RedX (Jackson ImmunoResearch Laboratories)) were all used at 1:200. DAPI (4',6-diamidino-2-phenylindole; Thermo Fisher Scientific) at 1:3,000 was used to stain DNA.

2.10 Titration of *C. trachomatis* stocks

Initially, 1x10^5 HeLa cells were seeded into each well of a 24-well plate with coverslips and incubated overnight at 37°C in the presence of 5% (v/v) CO_2. The next day, the chlamydial strain to be titrated was thawed and four 10-fold serial dilutions in a volume of 500 µl were done in HBSS. Then, 200 µl of the dilution was added to each well, which had been pre-washed with HBSS, and this was incubated for 30 min at 37°C in a humidified atmosphere containing 5% (v/v) CO_2. Following this, the inoculum was removed, and DMEM with 10% (v/v) FBS and 10 µg/ml gentamicin was added. The infected cells were incubated for 24 h at 37°C in a humidified atmosphere containing 5% (v/v) CO_2. The cells were then fixed with methanol and immunolabeled with antibody anti-CT-FITC. The equation below was utilized to calculate the inclusion forming units (IFUs) per ml (Scidmore, 2005):

$$IFU/ml = \frac{Nº\ of\ fields/coverslip^* \times Dilution\ factor \times Average\ nº\ of\ inclusions\ /field}{Volume}$$

*=774.47 (using the 40x objective of Zeiss AxioImager D2 fluorescence microscope)

2.11 Infection of HeLa 229 cells with *C. trachomatis*

The procedure for infecting mammalian cells with *C. trachomatis* was carried out as previously outlined (da Cunha et al., 2017). In short, HeLa cells were seeded a day prior to the infection in the suitable format (either multi-well plates or flasks) for tissue culture. The day of infection, the plate or flask was rinsed with HBSS, and *C. trachomatis* inoculum was prepared in SPG or HBSS and added to the cells. The cells were incubated for 30 min at 37°C in a humidified atmosphere containing 5% (v/v) CO_2 (multi-well plates) or 60 min at room temperature with gentle rocking (flasks). Next, the inoculum was removed and exchanged by DMEM with 10% (v/v) FBS along with 10 µg/ml gentamicin and/or the appropriate antibiotic. This marked the beginning of the infection, i.e. time zero of infection.

2.12 Western Blot

HeLa cells previously seeded at 1 x 10^5 cells/well at 24-well plate were infected at a multiplicity of infection (MOI) of 1.5 and incubated at 37°C in a humidified atmosphere containing 5% (v/v) CO_2 for 40 h. Following that, the pellet of the infected and trypsinized HeLa cells was obtained after a centrifugation at 2.200 x g for 5 min. The pellet was then washed twice with ice-cold PBS and then resuspended with SDS-PAGE loading buffer [50 mM TrisHCl 50 mM, pH 6.8, 2.0% (w/v) SDS, 10% (v/v) glycerol, 0.1 M β-mercaptoethanol, 0.1% (w/v) bromophenol blue] to which 0.7µl of benzonase (Novagen) was added. After an incubation of 10 min for the benzonase to act, the proteins in the cell extracts were separated using a 12% SDS-PAGE gel. Subsequently, the proteins were transferred to a nitrocellulose membrane (Bio-Rad). The membrane was blocked with blocking buffer containing 4% (w/v) dried skimmed milk in PBS with 0.1% (w/v) Tween-20. Following blocking, the membrane was incubated with primary antibodies overnight. After washing with PBS containing 0.1% (w/v) Tween-20, the membrane was incubated during 1 h with horseradish peroxidase-conjugated secondary antibodies. The SuperSignalTM West Pico Chemiluminescent Substrate (Thermo Fisher Scientific) by exposure to Amersham Hyperfilm ECL (GE Healthcare) was used to detect the target proteins

2.13 Bacterial Two-Hybrid (BACTH) assay

For the BACTH assays, each strain of *E. coli* BTH101 strain transformed with the generated or control plasmids was inoculated on LB with ampicillin and kanamycin (three colonies from each strain) and incubated overnight at 37°C with shaking (150 rpm). Then, the OD_{600} was measured. If the OD_{600} value exceeded 1.5, 5 µL of the culture was transferred, but if the OD_{600} value was less than 1.5, the volume was adjusted to correspond to an OD_{600} of 1.5. These volumes were then transferred to a LB plate containing X-Gal (40 µg/mL), 0.5 mM IPTG, 100 µg/mL ampicillin and 50 µg/mL kanamycin, and the plate was incubated for 3 to 4 days, at 30°C.

2.14 Statistical analysis

Statistical analyses were done using GraphPad Prism version 9.3.1 for Windows, GraphPad Software, www.graphpad.com. Three or more independent replicates were performed for all data analyzed. Differences were considered significant only when the p-value was less than 0.05.

3

RESULTS

3.1 *C. trachomatis* CT195 and CT214 proteins are bona fide Incs

To analyze the production and localization of putative *C. trachomatis* Incs CT195 and CT214, we used two previously constructed plasmids (pML39 and pML33; Table A. 3 in Annexes) harbouring *ct195* and *ct214* in frame with the sequence encoding a double hemagglutinin (2HA) tag and under the control of their respective endogenous promoters (Figure 3.1A). These two plasmids were used to transform *C. trachomatis* L2/434 and the presence of the plasmids in the resulting strain was confirmed by PCR (Figure 3.1B). HeLa cells were then infected for 40 h by these two strains. Immunoblotting from extracts of the infected cells revealed the production of proteins showing a migration on SDS-PAGE compatible with the predicted molecular mass of CT195-2HA (~43 kDa) and CT214-2HA (~62 kDa) (Figure 3.1C). Overall, this confirmed that the generated *C. trachomatis* strains produced the desired putative Incs.

To verify if CT195 and CT214 are bona fide Incs, HeLa cells were infected for 16, 24 and 40 h with the two *C. trachomatis* strains producing CT195-2HA or CT214-2HA. The infected cells were fixed and analysed by immunofluorescence microscopy. This revealed that both CT195-2HA and CT214-2HA appeared at the periphery of the inclusion, indicating that they localize at the inclusion membrane (Figure 3.1D and E). Furthermore, CT214-2HA also appeared in puncta at the inclusion membrane (Figure 3.2A), indicating it could localize at inclusion microdomains (Mital et al., 2010). Therefore, CT195 and CT214 are bona fide Incs, i.e., they possess bilobal transmembrane regions (Figure 1.3) and they localize at the inclusion membrane.

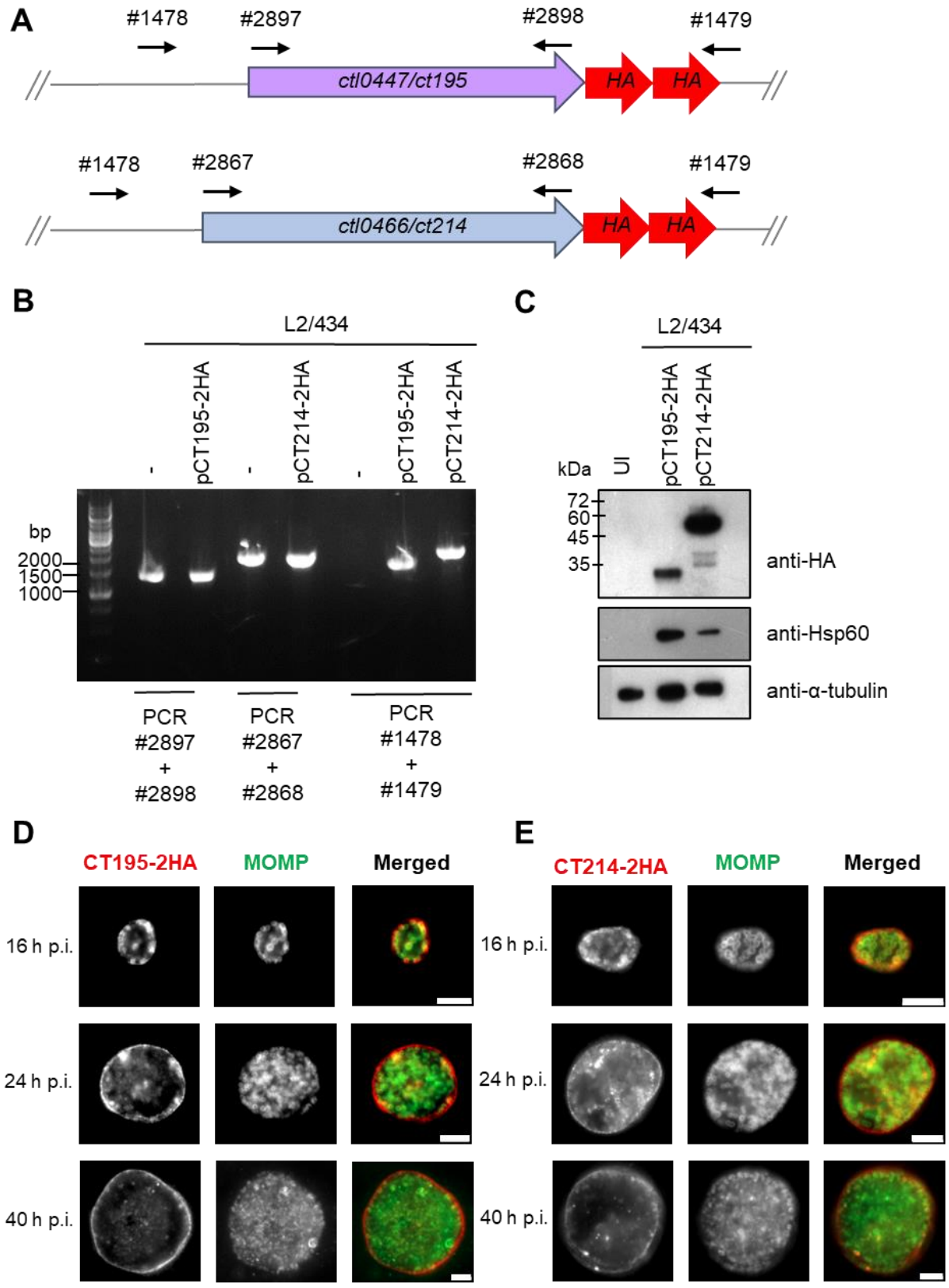

Figure 3.1. The *C. trachomatis* CT195 and CT214 proteins localize in the inclusion periphery. (A) Representation of the segment of plasmids (pCT195-2HA/pML39 or pCT214-2HA/pML33) carrying the *ctl0447/ct195* and *ctl0466/ct214* genes in frame with the sequence encoding a double hemagglutinin (2HA) to allow detection of the encoded proteins by immunoblotting and immunofluorescence microscopy. The numbers and

arrows indicate the primers and their orientation used in PCR reactions to confirm the presence of the desired genes. (B) Agarose gel showing the result from PCRs with the indicated primers and DNA templates. (C - E) HeLa cells were left uninfected (UI) and/or infected for 16, 24 and/or 40 h with *C. trachomatis* L2/434 harbouring pCT195-2HA or pCT214-2HA. (C) Whole cell lysates were analyzed by immunoblotting with antibodies against HA. For bacterial and host cell loading controls antibodies against *C. trachomatis* Hsp60 and human α-tubulin, respectively, were used. (D and E) The cells were fixed with methanol and immunolabeled with anti-HA (red) and anti-*C. trachomatis* major outer membrane protein (MOMP; green) antibodies and appropriate fluorophore-conjugated secondary antibodies. Then, cells were observed by fluorescence microscopy. Scale bars, 5 µm.

3.2 *C. trachomatis* Inc CT214 localizes in microdomains at the inclusion membrane throughout infection of HeLa cells

Several Incs have been shown to localize at inclusion microdomains (Weber et al., 2015). For example, we recently showed that *C. trachomatis* IncM localizes transiently at inclusion microdomains from 12 to 20 h p.i. (Luís et al., 2023). Contrary to what has been described for other Incs that localize at inclusion microdomains, IncM patches at the inclusion membrane are not consistently near the host cell centrosome (Luís et al., 2023).

To confirm and characterize the localization of CT214 at the inclusion microdomains, HeLa cells were infected for 16, 24 and 40 h with the *C. trachomatis* strain producing CT214-2HA. The infected cells were fixed and analysed by immunofluorescence microscopy. This confirmed that CT214-2HA localized at specific regions within the inclusion membrane at a frequency of 53 ± 11% (16 h p.i.), 34 ± 6% (24 h p.i.), and 36 ± 7% (40 h p.i.) (Figure 3.2A). Therefore, while IncM localizes transiently at inclusion microdomains (Luís et al., 2023), the localization of CT214 at these specific regions can be observed throughout the chlamydial infectious cycle.

To analyse the possible co-localization of CT214 and IncM at microdomains, HeLa cells were infected for 16 h with the *C. trachomatis* strain producing CT214-2HA. At this time-point, IncM can be found at microdomains (Luís et al., 2023). The infected cells were fixed and analysed by immunofluorescence microscopy using anti-HA antibodies to detect CT214-2HA and anti-IncM antibodies to detect endogenous IncM. This revealed that CT214-2HA microdomains co-localized at a frequency of 66 ± 6% with IncM microdomains (Figure 3.2B). Thus, most CT214-2HA microdomains co-localized with IncM microdomains.

Finally, to analyse the possible proximity between CT214-2HA microdomains and host cell centrosomes, HeLa cells were infected for 16, 24, and 40 h with the *C. trachomatis* strain producing CT214-2HA. The infected cells were fixed and analysed by immunofluorescence microscopy using anti-γ-tubulin antibodies to label the centrosome. The proximity of CT214-2HA microdomains to centrosomes was assessed by using the Fiji software (Schindelin et al., 2012), enumerating microdomains within 1 µm of the nearest centrosome (Figure 3.2C). This revealed that 46 ± 5% (at 16 h p.i.), 50 ± 1% (at 24 h p.i.), and 31 ± 7% (at 40 h p.i.) of CT214-2HA microdomains localized near the host cell centrosome (Figure 3.2D).

In summary, these experiments confirmed that CT214 localizes at inclusion microdomains. Differently from IncM (Luís et al., 2023), but accordingly to what has been described for other Incs (Mital et al., 2010), CT214 could be found at inclusion microdomains throughout the chlamydial infectious cycle and often near the host cell centrosome.

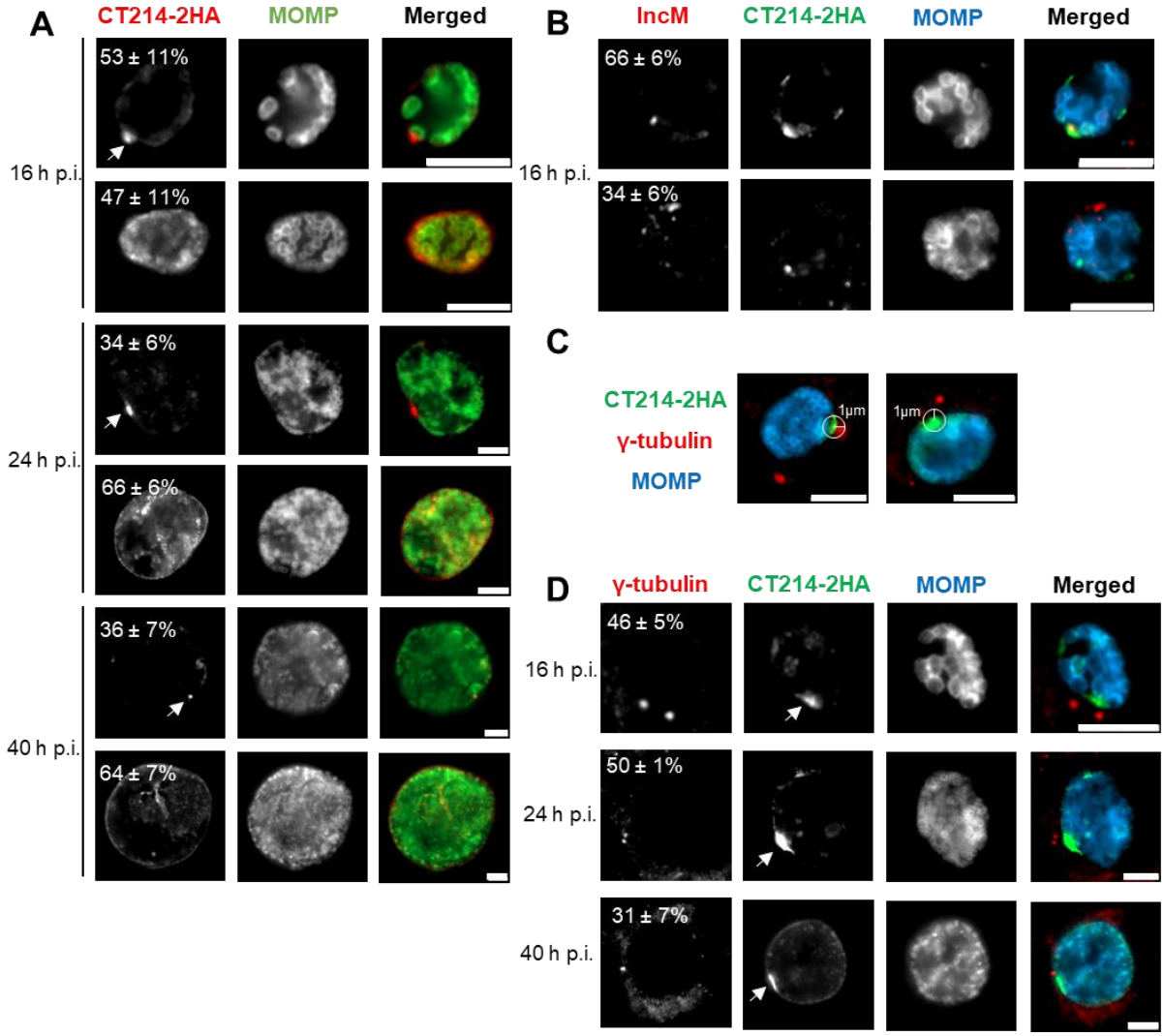

Figure 3.2. The *C. trachomatis* CT214 protein localizes in microdomains in the inclusion membrane. HeLa cells were infected for 16, 24 and 40 h with *C. trachomatis* L2/434 harbouring pCT214-2HA. Then, the cells were fixed with methanol. (A) The cells were immunolabeled with anti-HA (red) and anti- *C. trachomatis* major outer membrane protein (MOMP; green) antibodies and appropriate fluorophore-conjugated secondary antibodies and observed by fluorescence microscopy. The values within the images indicate the percentage of infected cells at each time point showing CT214-2HA at inclusion microdomains (indicated by a white arrow) or uniformly around the inclusion. The values are the average of four independent experiments ± standard error of the mean (SEM). (B) The cells were immunolabeled with anti-IncM (red), anti-HA (green) and anti-MOMP (blue) antibodies and appropriate fluorophore-conjugated secondary antibodies and observed by fluorescence microscopy. The values within the images indicate the percentage of infected cells showing colocalization between IncM and CT214-2HA at inclusion microdomains (upper panel) or no colocalization (lower panel). The values are the average of three independent experiments ± SEM. (C and D) The cells were immunolabeled with anti-γ-tubulin (red), anti-HA (green) and anti-MOMP (blue) antibodies and appropriate fluorophore-conjugated secondary antibodies and observed by fluorescence microscopy. (C) Illustration of the procedure used to evaluate if CT214-2HA inclusion microdomains are within 1 µm of the nearest centrosome. (D) The values within the images indicate the percentage of infected cells at each time point showing CT214-2HA inclusion microdomains within 1 µm of the nearest centrosome. The values are the average of three or four independent experiments ± SEM. Scale bars, 5 µm.

3.3 Analysis of possible homotypic Inc-Inc interactions

The co-localization of IncM and CT214 microdomains at 16 h p.i. led us to aim to investigate whether these two proteins can interact with each other. To do so, we aim to perform a bacterial two-hybrid (BACTH) assay (Battesti & Bouveret, 2012). Previous studies have shown that the BACTH system is a valuable approach for analyzing Inc-Inc interactions (Gauliard et al., 2015).

Briefly, the BACTH system is based on reconstituting the activity of adenylate cyclase, an enzyme involved in cAMP (cyclic AMP) synthesis, through the interaction of two proteins, in an *E. coli cya* strain. It uses the catabolic domain of adenylate cyclase from *Bordetella pertussis*, which consists of two complemented fragments (T18 and T25). These fragments when fused to polypeptides that interact with each other, leads to functional complementation between the fragments, thereby restoring cAMP synthesis. This re-establishes the cAMP signalling cascade, leading to the expression of catabolic genes, including those in the *lac* and *mal* operons. Bacteria with this system can use lactose or maltose as their only carbon source, enabling growth on specific indicator (e.g. LB-X-gal) or selective media (Karimova et al., 1998).

To test the system, similar to previous studies, we used IncA as a model (Gauliard et al., 2015), because this protein exhibits oligomerization properties (Delevoye et al., 2004). For this, we generated plasmids encoding T18-IncA-2HA and His-T25-IncA (Figure 3.3A). Essentially, these are the same plasmids that were used before to test the homotypic IncA-IncA interaction except that in our constructs IncA was tagged with C-terminal 2HA and in the T25 fragment was tagged with a N-terminal His-tag.

Subsequently, we co-transformed these plasmids, along with empty plasmids (pUT18 and pHis-pKT25), into *cya* deficient *E. coli* BTH101, generating four strains (Fig. 3A): producing T18-IncA-2HA and His-T25-IncA; producing T18-IncA-2HA and carrying plasmid pHis-pKT25; carrying plasmid pUT18 and producing His-T25-IncA; carrying plasmids pUT18 and pHis-pKT25. These strains, along with an available positive control (producing T18-zip and T25-zip, where zip is a 35-resideus-long leucine zipper), were plated on specific indicator plates (Figure 3.3A).

As shown in Figure 3.3B, only the positive control yielded a protein-protein interaction (blue color in the indicator plates), indicating that the two fusion proteins, His-T25-IncA and T18-IncA-2HA, did not associate in *E. coli* in these conditions. Since we did not obtain the expected result with the IncA-IncA interaction, we decided not to proceed with using BACTH to analyze the possible interaction between CT214 and IncM, because of time constraints and further developments of the work and the inability to detect an interaction between these proteins would render further results inconclusive.

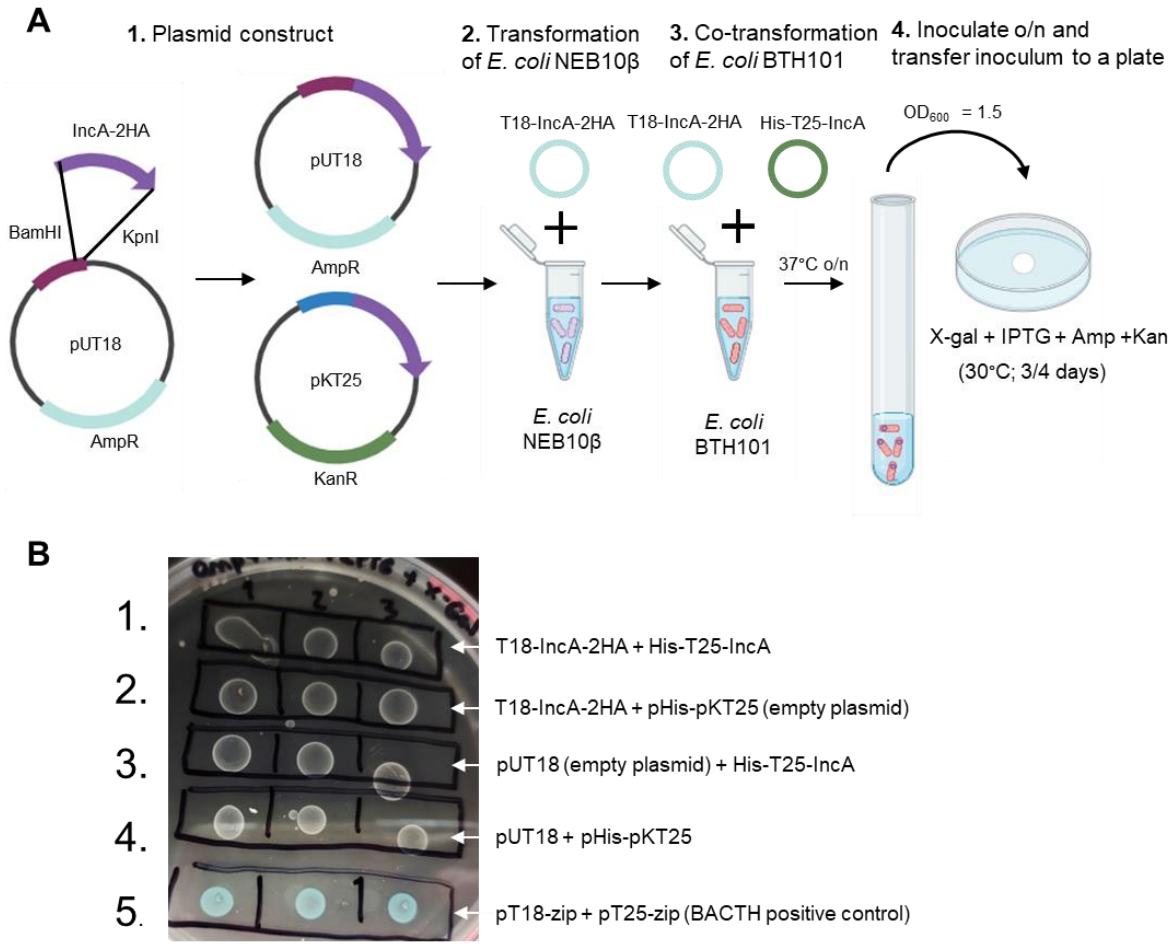

Figure 3.3. Bacterial two-hydrid (BACTH) analysis of possible homotypic Inc-Inc interactions using IncA as model. (A) Schematic representation of the procedure used to generate plasmids encoding IncA and test for possible IncA-IncA interactions by BACTH. Initially, the plasmids were constructed using *E. coli* NEB10β as cloning host strain. After confirming plasmid accuracy, the BACTH reporter strain *E. coli* BTH101 was co-transformed with both plasmids (and also with control plasmids), as indicated. Afterwards, three colonies of each strain were grown overnight and at least an optical density at 600 nm (OD_{600}) of 1.5 was spotted on a LB plate supplemented with X-gal (40 µg/mL), IPTG (0.5 mM) and selective antibiotics (ampicillin – Amp; kanamycin – Kan). (B) Illustrative result of a BACTH assay: 1. T18-IncA-2HA + His-T25-IncA; 2. T18-IncA-2HA + pHis-pKT25 (empty plasmid); 3. pUT18 (empty plasmid) + His-T25-IncA; 4. pUT18 + pHis-pKT25; 5. pT18-zip + pT25-zip (BACTH positive control).

3.4 Generation of *C. trachomatis ct195::aadA* mutant strain

To understand the roles of CT195 and CT214 during the *C. trachomatis* infectious cycle, we aimed to generate *C. trachomatis ct195* and *ct214* mutant strains. Using pDFTT3aadA (Table A. 3 in Annexes) as the backbone plasmid, we constructed *ct195* and *ct214* mutator plasmids using the TargeTron™-based strategy (Key & Fisher, 2016). Using this approach, we retargeted the intron in the backbone plasmid for *ct195* and *ct214* disruption (between nucleotides 160 and 161 for *ct195*; 301 and 302 for *ct214*), resulting in plasmids pAB1 and pAB2 (Table A. 3 in Annexes), respectively. These plasmids were used to transform *C. trachomatis* L2/434 wild-type strain (Figure 3.4A). At 16 h p.i., spectinomycin was added to select the mutant strains. At 48 h p.i., the cells were osmotically lysed, and the resulting supernatant containing the mutant strains was used to re-infect cells with spectinomycin in the medium.

This process was repeated to expand the mutant strain until a monolayer of infected cells was observed by phase-contrast light microscopy (Figure 3.4A). We successfully obtained the *C. trachomatis ct195::aadA* mutant strain, but were unable to generate the *ct214::aadA* mutant strain. Therefore, the characterization of the *ct195::aadA* mutant strain was the main focus of the subsequent work and CT214 was not further analysed.

To confirm the disruption of *ct195* by PCR, DNA primers specific to the intron, gene, and a combination of these were used (Figure 3.4B). The size or presence of bands obtained using these DNA primers was then compared between reactions using as template the chromosomal DNA of strains L2/434 and *ct195::aadA* mutant, and plasmid pAB1. This allowed us to conclude that the intron targeted ct195 (Figure 3.4C) The insertion of the intron at the correct region was further confirmed by DNA sequencing.

After obtaining the mutant strain and confirming the correct insertion of the intron, it was necessary to isolate clones of this strain by plaque purification. As *C. trachomatis* is an obligate intracellular bacterium, it cannot be isolated on agar plates like other bacteria. Instead, plaque formation on a monolayer of cells was used to isolate the mutant strain clones. After obtaining two plaques, they were expanded and one of the clones was titrated and used in subsequent experiments (Figure 3.4A).

We then transformed the *C. trachomatis ct195::aadA* mutant strain with a chlamydial expression plasmid encoding CT195-2HA (pML39; Table A. 3 in Annexes), which enabled the generation of a *ct195* complemented strain. The strain was confirmed by PCR using DNA primers specific to *ct195* and the 2HA tag present in pML39. The presence of bands obtained using these DNA primers was then compared between PCR reactions using as template the chromosomal DNA of strains L2/434, and *ct195::aadA* carrying pML39, and plasmid pML39 (Figure 3.4D). The complemented strain, which was not plaque purified, was then titrated to be used in the subsequent work.

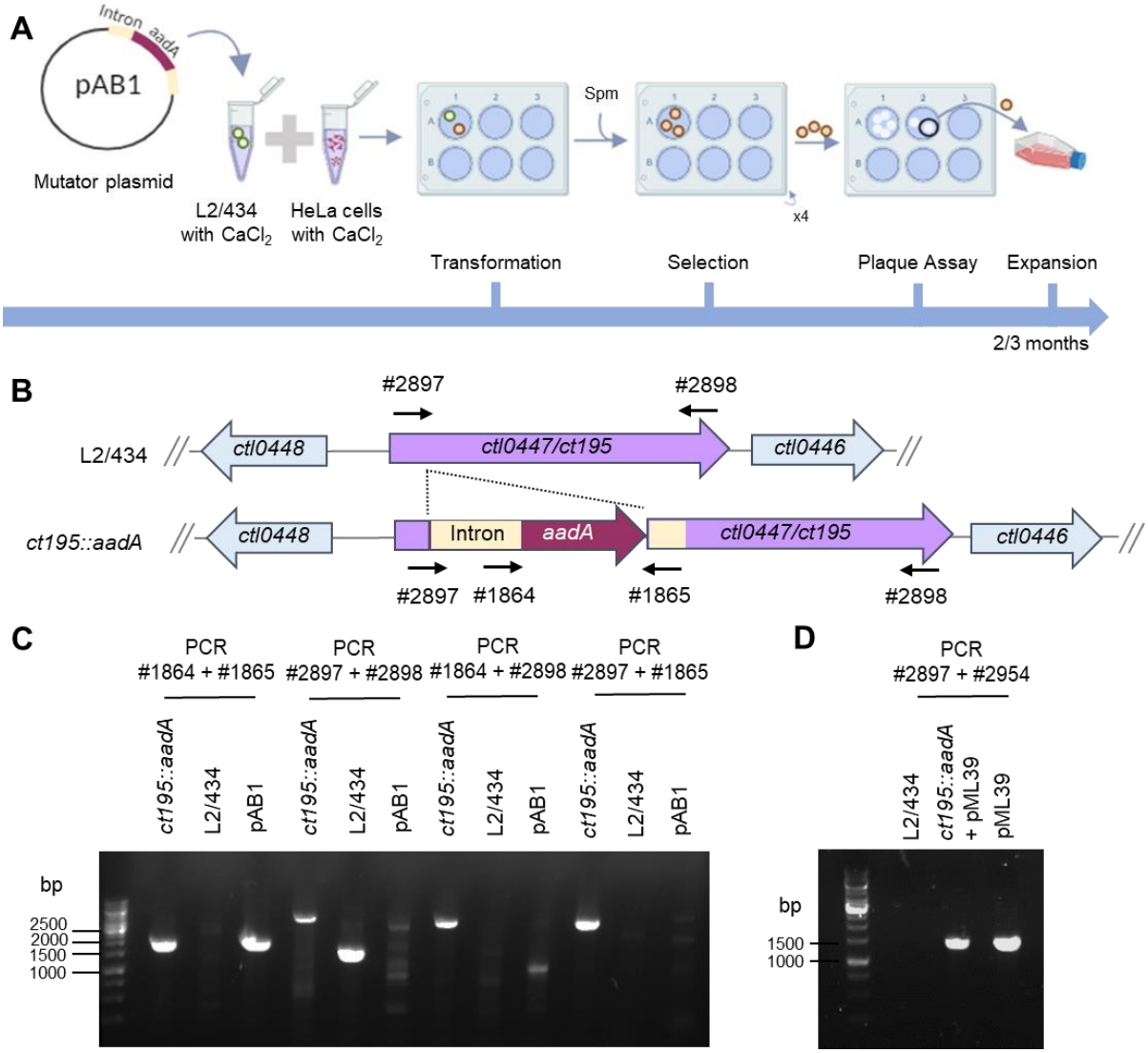

Figure 3.4. Generation of C. trachomatis *ct195*::*aadA* mutant strain and its complemented strain. (A) Schematic representation of the procedure used to obtain *C. trachomatis ct195::aadA* mutant strain. Initially, the mutator plasmid (pAB1) carrying an intron targeting *ct195* (TargetTron) was used to transform the *C. trachomatis* L2/434 strain. Several passages in the presence of the selective antibiotic (spm, spectinomycin) were performed until the mutant strain was obtained. Afterwards, two clones of the *ct195::aadA* mutant strain were isolated using the plaque assay procedure. The clonal strains obtained were further expanded to obtain chlamydial stocks and then titrated. Only one of the clones was subsequently used. (B) Representation of the locus of *ctl0447* (orthologue of *ct195* in strain D/UW3) in L2/434 and in the resulting mutant (*ct195::aadA*) strain, obtained by inserting a modified group II intron carrying the gene that confers spectinomycin resistance (*aadA*). (C) Agarose gel showing the results of PCRs done using the indicated primers and DNA templates; bp, base pairs. (D) To obtain the complemented strain, *C. trachomatis ct195::aadA* was transformed with plasmid pML39 encoding CT195-2HA. After selection, expansion and clonal isolation, as detailed above for the *ct195::aadA* mutant, the resulting strain was verified by PCR using one primer specific to the gene (#2897) and the other to the hemagglutinin tag (#2954) and the indicated DNA templates; bp, base pairs.

3.5 Presence of CT195 reduces the intracellular growth *C. trachomatis* in tissue culture cells

To analyse a possible role of CT195 in the intracellular growth of *C. trachomatis*, HeLa cells were infected for 24 and 48 h with a MOI of 0.1 with the parental *C. trachomatis* L2/434 strain, the *ct195::aadA* mutant strain, and the *ct195::aadA* complemented strain (Figure 3.5A). Considering that each inclusion formed during infection represents one inclusion forming unit (IFU), we measured infectivity as an indicator of intracellular growth. This was done by fixing cells, immunolabelling for chlamydiae and enumerating the number of inclusions by fluorescence microscopy. The infectivity at 24 h corresponded to the actual IFUs that were used to infect the cells at both time points, referred to as the Input. The progeny obtained from the 48-h infection was collected by cell lysis and used to infect HeLa cells. The infectivity obtained from this infection is referred to as the Output (Figure 3.5A). To compare the intracellular growth between each strain, the Output:Input ratio was calculated, ensuring that the differences in the intracellular growth were due to the strains themselves and not due to differences in the initial IFUs used. Additionally, to better visualize the differences between each strain and to avoid being influenced by variations between experimental replicates, each ratio was normalized by dividing it by the Output:Input ratio of the L2/434 strain.

The *ct195::aadA* mutant showed a significantly greater (~1.5-fold) output/input ratio relative to the L2/434 strain (Figure 3.5B). Moreover, this was reverted by introducing the intact *ct195* gene in the mutant strain as the complemented strain did not show a significant difference in the output/input ratio relative to the L2/434 strain (Figure 3.5B). Therefore, expression of *ct195* limits *C. trachomatis* growth.

To determine if the increased intracellular growth of the *ct195::aadA* mutant strain was related to a larger inclusion area, we measured this parameter in cells infected by *C. trachomatis* L2/434, *ct195::aadA* mutant or the complemented strain for 24 and 48 h p.i. The infected cells were then fixed and immunolabeled and stained (Figure 3.5C). This revealed that both at 24 or 48 h p.i. the mutant and complemented strains did not show any significant differences in inclusion area compared to the inclusions of the L2/434 strain (Figure 3.5D). Therefore, although CT195 limits chlamydial growth this does not have an impact in the inclusion area. While somewhat surprising, previous studies showed that the size of the inclusion size is not necessarily a direct measure of chlamydial growth (Engström et al., 2015).

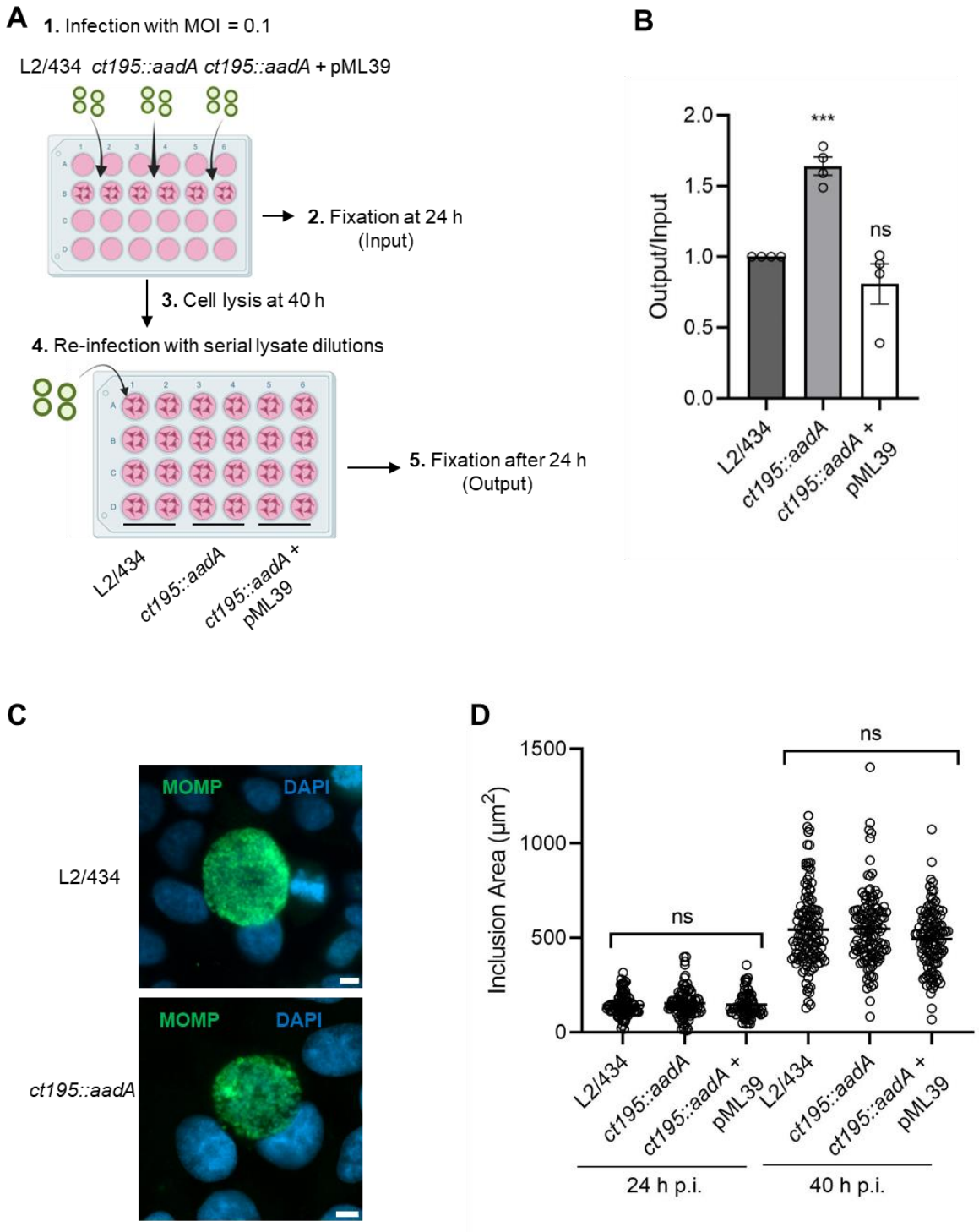

Figure 3.5. The *ct195::aadA C. trachomatis* mutant strain exhibits higher intracellular growth than the wild-type L2/434 strain. HeLa 229 cells were infected with *C. trachomatis* L2/434, *ct195::aadA* or *ct195::aadA* harbouring pML39 for 24 or 40 h at a multiplicity of infection of 0.1. To measure the inclusion area, the cells were fixed with methanol at both time-points. For assessing intracellular growth, the infected cells were also fixed with methanol at 24 h p.i., while the cells infected for 40 h were lysed and then the released infectious particles were used to re-infect HeLa 229 cells for 24 h, after which they were fixed with methanol. For assessing intracellular growth, the cells fixed at 24 h in the primary and secondary infections were immunolabeled with anti-*C. trachomatis* fluorescein isothiocyanate (FITC). (A) Schematic representation of the procedure used to monitor chlamydial intracellular growth. (B) The infectivity of each strain was determined by measuring inclusion forming unit (IFUs)/mL,

resulting in two values (Input and Output). For each strain, the Output/Input ratio was calculated and normalized by dividing it by the Output:Input ratio obtained for the L2/434 strain. (C) The cells were immunolabeled with anti-*C. trachomatis* major outer membrane protein (MOMP; green) antibodies and an appropriate fluorophore-conjugated secondary antibody, stained with DAPI and observed by fluorescence microscopy. Representative images of cells infected with *C. trachomatis* L2/434 or *ct195::aadA* mutant. Scale bars, 5 µm. (D) Using Fiji sofware, the area of at least 90 inclusions from three independent experiments was measured. Data, ± standard error of the mean from three or four independent experiments. P-values were obtained by one-way ANOVA and Dunnett's post-hoc test analysis relative to L2/434 strain, using GraphPad Prism version 9.3.1 for Windows, GraphPad Software, www.graphpad.com ; ns, not significant; *, $P < 0.05$; **, $P < 0.01$; ***, $P < 0.001$.

3.6 Presence of CT195 delays fusion between inclusions

During *C. trachomatis* infection of host cells, it is possible that more than one EB enters a host cell, leading to the formation of more than one early inclusion within that cell. Some species of *Chlamydia*, including *C. trachomatis*, exhibit homotypic fusion of these inclusions, resulting in a single large inclusion. It has been reported that IncA is involved this fusion process (Hackstadt et al., 1999).

Therefore, we investigated whether *ct195* influenced the fusion between inclusions. For this, HeLa cells were infected with *C. trachomatis* L2/434, *ct195::aadA* mutant or complemented strains, at different and greater than normal MOIs (0.6, 3.0 or 6.0), aiming to promote the infection of a single cell by multiple EBs. Then, the cells were fixed at 16 and 24 h, immunolabeled and stained, and analyzed by fluorescence microscopy to enumerate the infected cells with more than one inclusion (Figure 3.6).

Although a large variation between experiments was observed in cells infected at a MOI of 6.0 and fixed at 24 h p.i., those infected by the *ct195::aadA* mutant showed significantly fewer cells with more than one inclusion than those infected by the L2/434 strain (Figure 3.6). Moreover, at the same MOI and time-points, there were no significant differences in cells with more than one inclusion between cells infected with the complemented strain and the L2/434 strain (Figure 3.6). A similar trend was observed in cells infected with a MOI of 3.0 and fixed at 24 h p.i. and in cells infected with a MOI of 6.0 and fixed at 16 h p.i., but no significant differences were observed (Figure 3.6A). In summary, these experiments suggested that CT195 delays the homotypic fusion between inclusions.

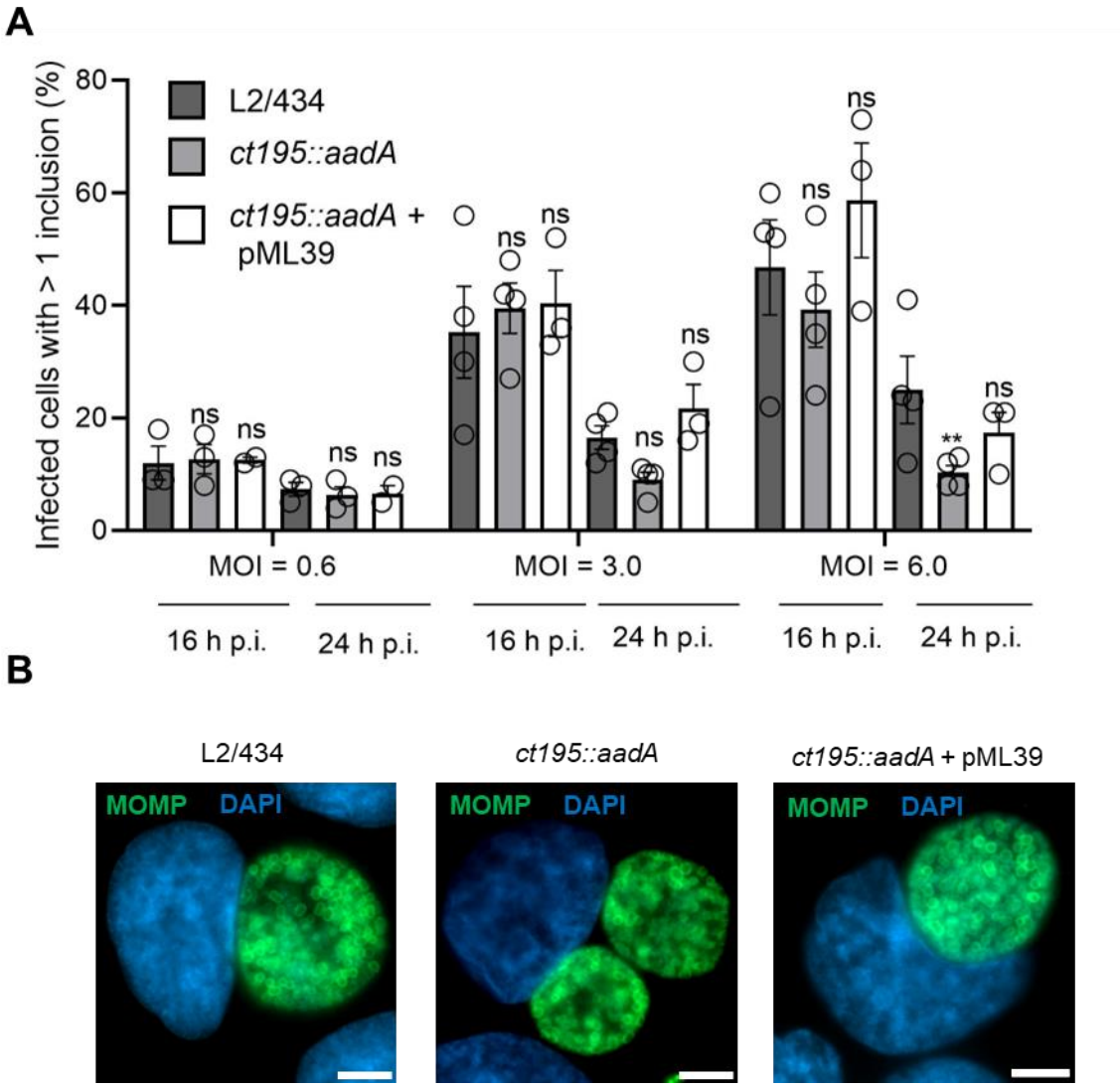

Figure 3.6. The inclusions of the *ct195::aadA C. trachomatis* mutant strain fuse faster than those of the wild-type L2/434 strain. HeLa cells were infected for 16 or 24 h with *C. trachomatis* L2/434, *ct195::aadA* or *ct195::aadA* harbouring pML39 (encoding CT195-2HA) at different multiplicities of infection (0.6, 3.0 or 6.0). Then, the cells were fixed with methanol and immunolabeled with anti-*C. trachomatis* major outer membrane protein (MOMP; green) antibody and appropriate fluorophore-conjugated secondary antibody and stained with DAPI. (A) Enumeration of the percentage of infected cells in which more than one inclusion was observed. Data, ± standard error of the mean from three or four independent experiments. P-values were obtained by two-way ANOVA and Dunnett's post-hoc test analysis relative to L2/434 strain, using GraphPad Prism version 9.3.1 for Windows, GraphPad Software, www.graphpad.com ; ns, not significant; *, $P < 0.05$; **, $P < 0.01$; ***, $P < 0.001$. (B) Representative image of a cell infected for 24 h with the *C. trachomatis* L2/434, *ct195::aadA* or *ct195::aadA* harbouring pML39 at a multiplicity of infection of 0.6, displaying one or two inclusions. Scale bars, 5 µm.

3.7 CT195 is not necessary for the ability of *C. trachomatis* to mediate redistribution of the Golgi complex and of the positioning of the host cell centrosome

Several Incs have been reported to affect various host cell processes that involve the cytoskeleton (Bugalhão & Mota, 2019), including centrosome positioning and the distributing of the Golgi complex. For example, in mammalian cells during interphase, the Golgi complex normally surrounds the centrosome, but in *C. trachomatis*-infected cells, the complex fragments and distributes around the inclusion (Heuer et al., 2008). This Golgi redistribution has been shown to be mediated at least by Incs InaC (Haines et al., 2021) and IncM (Luís et al., 2023). The inclusion is also normally positioned near the host cell centrosome (Bugalhão & Mota, 2019). Therefore, we investigated whether CT195 might be involved in the mispositioning of centrosomes or affect the distribution of the Golgi complex during C. trachomatis infections of host cells. For this, HeLa cells were left uninfected or were infected with *C. trachomatis* L2/434 or *ct195::aadA* mutant for 24 or 48 h. Then, they were fixed, immunolabelled and stained, and analyzed by fluorescent microscopy. Using the Fiji software (Schindelin et al., 2012), we measured the length of Golgi distribution around the inclusion, distance from the centrosomes to the closest point of the inclusion and to the nucleus, and the distance between centrosomes. This analysis revealed no significant differences between the length of Golgi distribution in cells infected by the L2/434 or the *ct195::aadA* mutant strain (Figure 3.7).

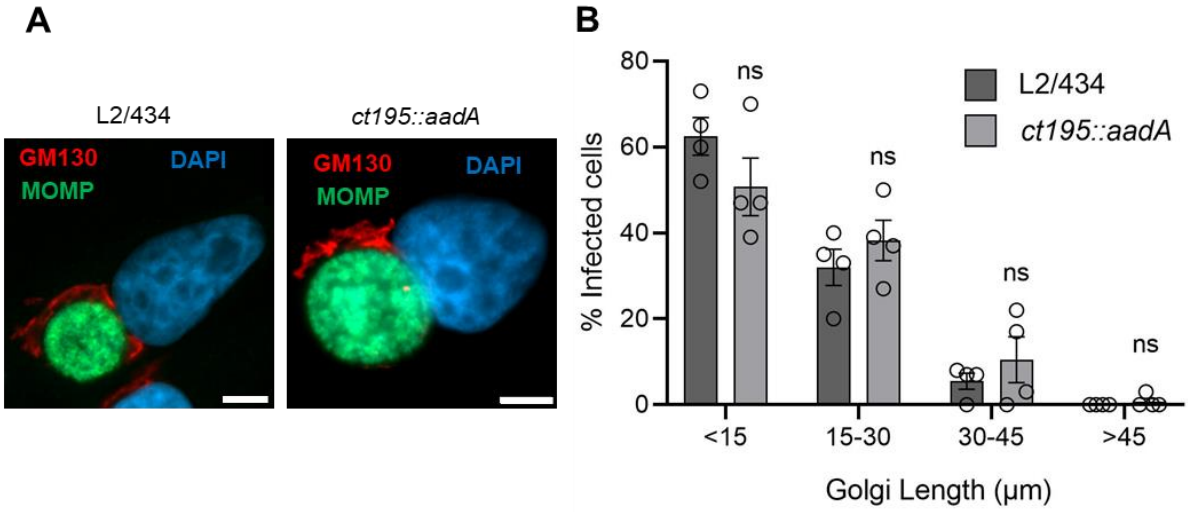

Figure 3.7. *C. trachomatis* CT195 is not required for Golgi complex redistribution or centrosome positioning. HeLa cells were infected for 24 h with *C. trachomatis* L2/434, *ct195::aadA* or *ct195::aadA* harbouring pML39 (encoding CT195-2HA) at a multiplicity of infection of 0.6. The cells infected were fixed with 4% (w/v) paraformaldehyde and immunolabeled with anti-*C. trachomatis* major outer membrane protein (MOMP; green) and anti-GM130 (red) antibodies and appropriate fluorophore-conjugated secondary antibodies, stained with DAPI, and analyzed by fluorescence microscopy. (A) Representatives image of the distribution of the Golgi complex in cells infected by *C. trachomatis* L2/434 or *ct195::aadA* strains. Scale bars, 5 µm. (B) Length of Golgi distribution around the inclusion was measured using Fiji. Values represent mean ± standard error of the mean from three independent

experiments, in which the measurements were done in ≥ 25 cells per experiment. P-values were obtained by t test, using GraphPad Prism version 9.3.1 for Windows, GraphPad Software, www.graphpad.com ; ns, not significant.

Likewise, in the analyses of centrosome localization (Figure 3.8A), no significant differences were observed in the distance from the centrosomes to the inclusion (Figure 3.8B), to the nucleus (Figure 3.8C), or in the distance between centrosomes (Figure 3.8D) in cells infected by the L2/434 or the *ct195::aadA* mutant strain. However, there were significant differences detected in the distance between the centrosome to the nucleus (Figure 3.8C) and in the distance between centrosomes (Figure 3.8D) when comparing uninfected cells to cells infected by the L2/434 strain. This revealed the defects caused by *C. trachomatis* infection in the centrosome positioning.

We concluded that CT195 is not involved in the processes responsible for the redistribution of the Golgi complex or the mispositioning of centrosomes in cells infected by *C. trachomatis*.

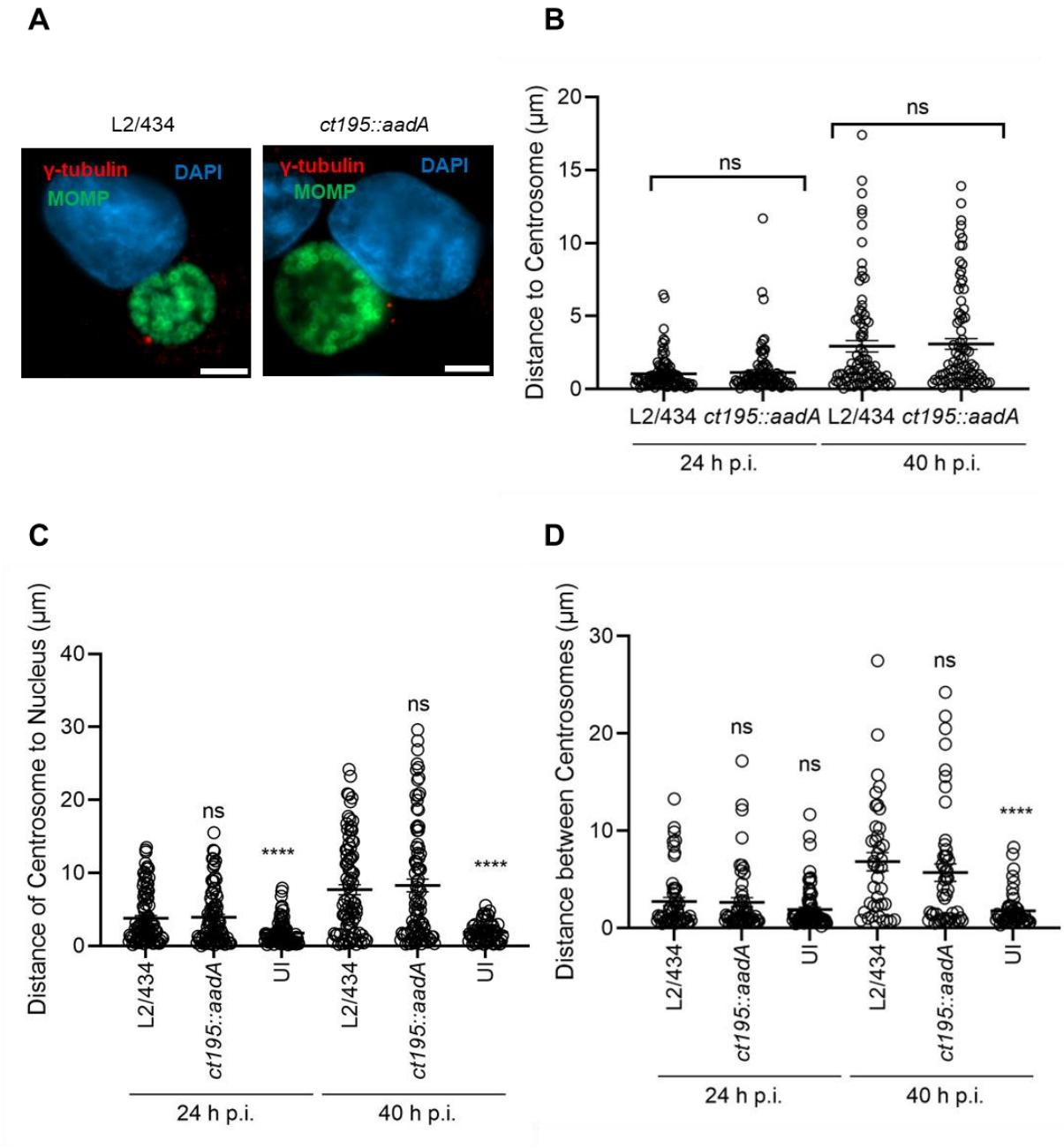

Figure 3.8. *C. trachomatis* CT195 is not required for modulation of centrosome positioning in infected cells. HeLa cells were left uninfected (UI) or infected for 24 or 40 h with *C. trachomatis* L2/434, *ct195::aadA* or *ct195::aadA* harbouring pML39 (encoding CT195-2HA) at a multiplicity of infection of 0.6. Then the cells were fixed with methanol and immunolabeled with anti-*C. trachomatis* major outer membrane protein (MOMP; green) and anti-γ-tubulin (red) antibodies and appropriate fluorophore-conjugated secondary antibodies, stained with DAPI, and analyzed by fluorescence microscopy. (A) Representative images of the localization of the host cell centrosome relative to the inclusion and nucleus in cells infected by *C. trachomatis* L2/434 or *ct195::aadA*. Scale bars, 5 µm. (B) The distance of the centrosomes to the closest point of the inclusion was measured by using Fiji. (C) The distance of the centrosomes to the closest point in the nucleus was measured using Fiji. (D) The distance between centrosomes was measured using Fiji. Each data represents three independent experiments, in which the measurements were done in ≥ 20 cells per experiment. P-values were obtained by t test, using GraphPad Prism version 9.3.1 for Windows, GraphPad Software, www.graphpad.com; ns, not significant; *, $P < 0.05$; **, $P < 0.01$; ***, $P < 0.001$.

3.8 CT195 contributes to multinucleation in *C. trachomatis*-infected host cells

C. trachomatis induces multinucleation in infected host cells (Greene, 2003; Brown et al., 2012) and IncM is involved in this process (Luís et al., 2023). To test if CT195 could also mediate host cell multinucleation, HeLa cells were left uninfected, or were infected with *C. trachomatis* L2/434, *ct195::aadA* mutant or the complemented strain for 24 and 48 h. Then, the cells were fixed and immunolabeled and stained. Subsequent fluorescence microscopy analysis revealed that at 40 h p.i. there were significantly less multinucleated cells in cells infected by the *ct195::aadA* mutant relative to those infected by the L2/434 strain (Figure 3.9). Moreover, cells infected by the complemented strain showed no difference in multinucleation relative to cells infected by the L2/434 strain. As in previous reports (Brown et al., 2014) (Luís et al., 2023), we also detected a significant difference in the number of multinucleated cells between *C. trachomatis* infected cells and uninfected cells. Therefore, CT195 also contributes to multinucleation in *C. trachomatis*-infected host cells suggesting that it inhibits host cell cytokinesis.

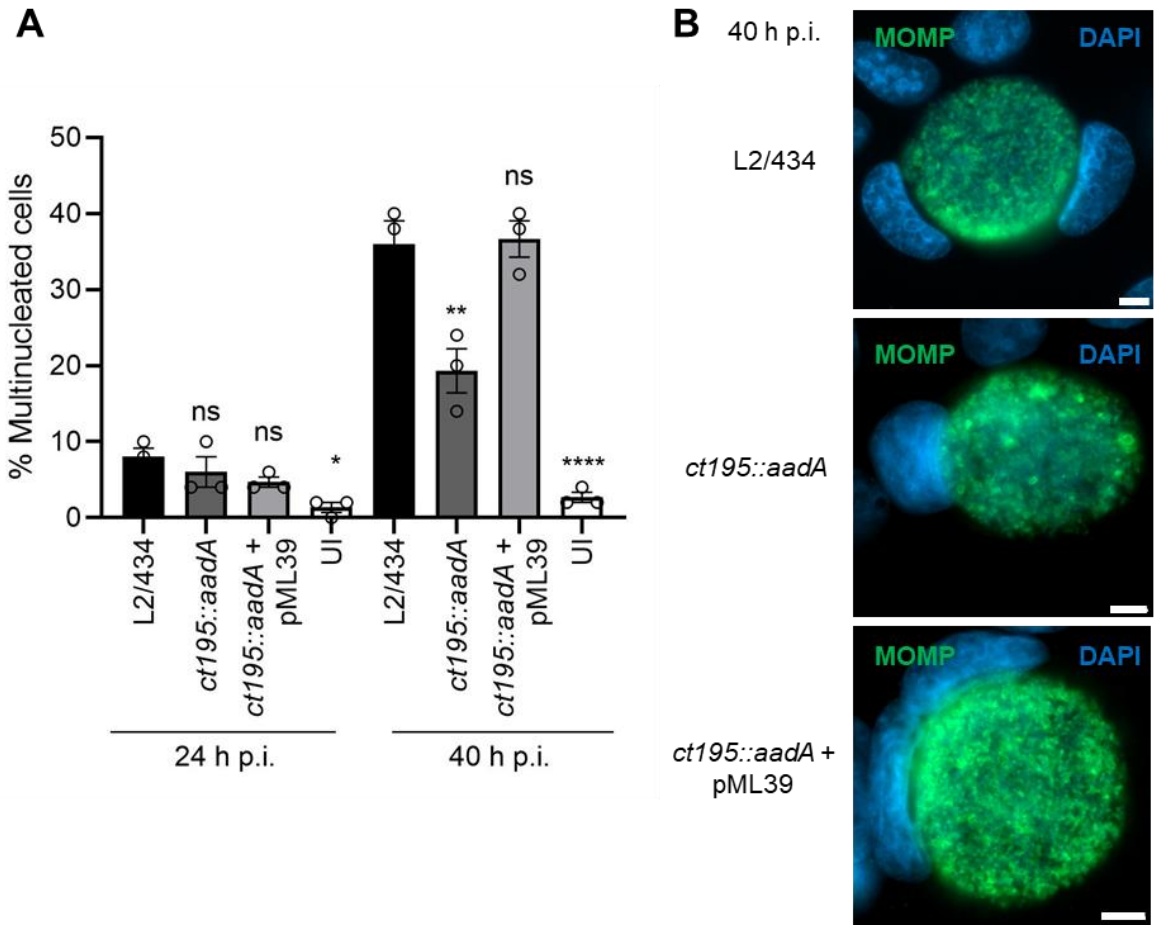

Figure 3.9. CT195 is involved in the ability of *C. trachomatis* to induce multinucleation in infected cells.

HeLa cells were left uninfected (UI) or infected for 24 or 40 h with *C. trachomatis* L2/434, *ct195::aadA* or *ct195::aadA* harbouring pML39 (encoding CT195-2HA) at a multiplicity of infection of 0.6. Afterwards, the cells were fixed using methanol and immunolabeled with anti-*C. trachomatis* major outer membrane protein (MOMP; green) antibody and appropriate fluorophore-conjugated secondary antibodies, stained with DAPI, and analyzed by fluorescence microscopy. (A) Enumeration of cells that exhibit more than one nucleus. Values represent means ± standard error of the mean, n = 3, 50 cells per experiment. P-values were obtained by one-way ANOVA and Dunnett's post-hoc test analysis relative to L2/434 strain, using GraphPad Prism version 9.3.1 for Windows, GraphPad Software, www.graphpad.com; ns, not significant; *, P < 0.05; **, P < 0.01; ***, P < 0.001. (B) Representative immunofluoresence microscopy images illustrating that cells infected by L2/434 or *ct195::aadA* harbouring pML39 display more multinucleated cells than those infected by the *ct195::aadA* strain. Scale bars, 5 µm.

3.9 The morphology of the inclusion is independent of CT195

We previously reported that IncM, which also contributes to multinucleation in *C. trachomatis*-infected host cells, plays a role in maintaining the normal morphology of the inclusion (Luís et al., 2023). Therefore, we analysed if CT195 is also required to control the morphology of the inclusion. For this, HeLa cells were infected by *C. trachomatis* L2/434 or the *ct195::aadA* mutant for 24 and 48 h. Following that, the infected cells were fixed and immunolabeled and stained. Then, the cells were analysed by fluorescence microscopy, and the circularity of the inclusions was calculated using Fiji (Schindelin et al., 2012). There were no significant differences observed between the circularity of the inclusions of the two strains at either time point (Figure 3.10). This indicates that CT195 has no role in the maintenance of the morphology of the inclusion in *C. trachomatis* infected cells.

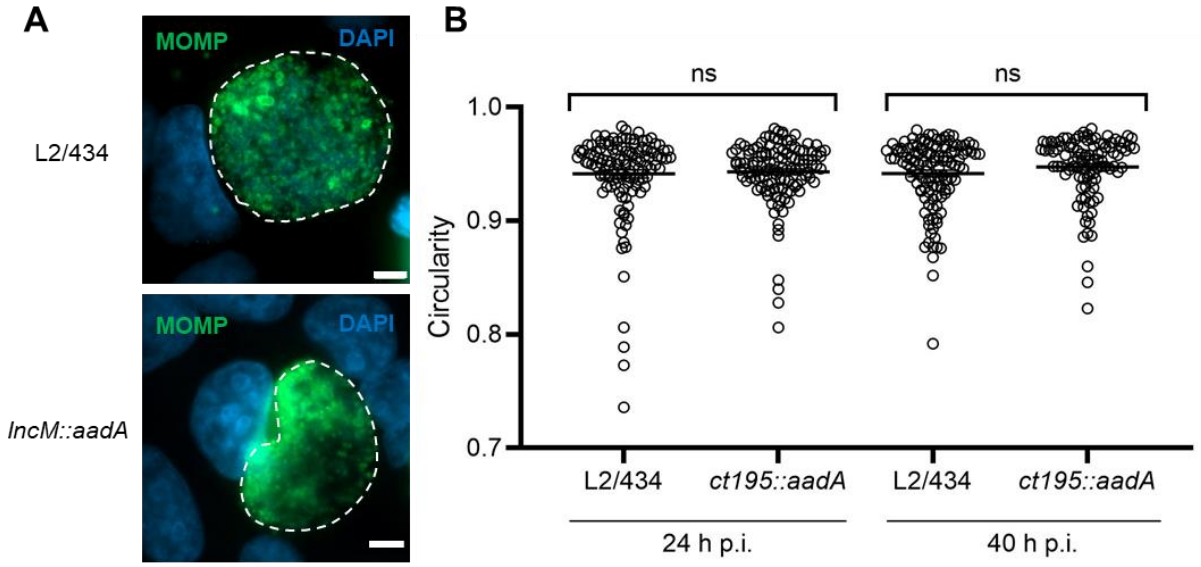

Figure 3.10. CT195 does not affect the morphology of the inclusion. (A) Illustrative image showing that the wild-type L2/434 inclusions are more circular than *C. trachomatis incM::aadA* mutant inclusions (images provided by Luís et al., 2023) . Scale bars, 5 µm. (B) HeLa cells were infected for 24 or 40 h with *C. trachomatis* L2/434 or *ct195::aadA* at a multiplicity of infection of 0.6. Then, the cells were fixed with methanol and immunolabeled with anti-*C. trachomatis* major outer membrane protein (MOMP; green) antibody and an appropriate fluorophore-conjugated secondary antibody, stained with DAPI, and analyzed by fluorescence microscopy. (B) Circularity was measured by Fiji using the following formula: 4p x (area/perimeter^2). A value of 1.0 represents a perfect circle; as this value decreases, it indicates that the shape becomes more of an elongated polygon. Values represent means ± standard error of the means, n = 3, ≥ 30 cells per experiment P-values were obtained by t test, using GraphPad Prism version 9.3.1 for Windows, GraphPad Software, www.graphpad.com; ns, not significant.

3.10 CT195 does not appear to be involved in the exit of EBs from host cells

Finally, a possible role of CT195 in chlamydial exit from host cells was investigated. For this, HeLa cells were infected with *C. trachomatis* L2/434, *ct195::aadA* mutant, complemented strain for 24, 48 and 72 h (Figure 3.11A). The 24-h time-point was used as a measure of infectivity, providing the actual IFUs used to infect the cells, which we refer as Input. As before, this was done by fixing cells, immunolabelling for chlamydiae and enumerating the number of inclusions by fluorescence microscopy (Figure 3.11A). The progeny obtained from the 48 and 70-h infection was collected from the culture supernatants without cell lysis and used to infect HeLa cells (Figure 3.11A). The infectivity obtained from both infections is referred as the Exit, providing the IFUs that exited the host at each collected time point.

To assess chlamydial exit differences among the strains, we calculated the Exit:Input ratio. This ensured that any variations in *Chlamydia* exit were solely attributable to the strains themselves, rather than differences in the initial IFUs used. Furthermore, to enhance clarity and mitigate the impact of experimental variability, we normalize each ratio by dividing It by the Exit:Input ratio of the L2/434 strain.

We observed that both the mutant and complemented strain exhibited an inconsistent behaviour relative to L2/434 (Figure 3.11B), This suggests that CT195 is not involved in mediating *C. trachomatis* exit from host cells, but further studies are required to conclude about this.

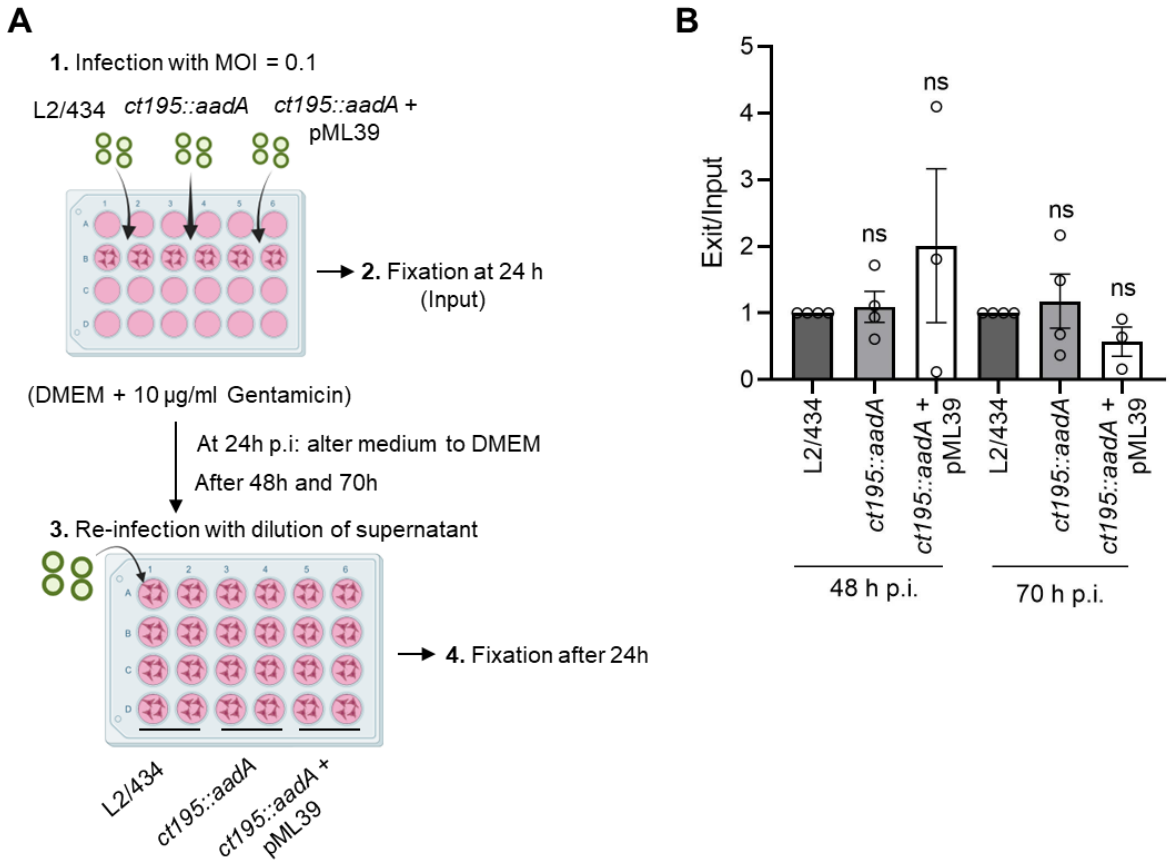

Figure 3.11. CT195 does not appear to be required for chlamydial exit from host cells. HeLa 229 cells were infected with *C. trachomatis* L2/434, *ct195::aadA* or *ct195::aadA* harbouring pML39 (encoding CT195-2HA) at a multiplicity of infection of 0.1 for 24, 48 or 70 h. The cells infected for 24 h were fixed with methanol. For the cells infected during 48 or 70 h, the supernatant was used to re-infect HeLa 229 cells for 24 h, after which it was fixed with methanol and immunolabeled with anti-*C. trachomatis* fluorescein isothiocyanate (FITC). (A) Schematic representation of the procedure used to measure the concentration (IFU/mL) of infectious chlamydiae that exit host cells between 24 and 48 h or 70 h p.i. (B) To assess chlamydial exit from host cells, the infectious particles present in culture supernatants were determined by measuring IFUs/mL at 48 and 70 h p.i. For each strain, the Exit/Input ratio was calculated and normalized by dividing it by the Exit:Input ratio of L2/434 (Input values was previously measured in this work). Values represent means ± standard error of the mean, n = 3. P-values were obtained by one-way ANOVA and Dunnett's post-hoc test analysis relative to L2/434 strain, using GraphPad Prism version 9.3.1 for Windows, GraphPad Software, www.graphpad.com; ns, not significant.

4

DISCUSSION

In this work, we identified two bona-fide *C. trachomatis* Incs (CT195 and CT214) by studying their subcellular localization in *Chlamydia*-infected. This was followed by aiming to functionally characterize them. This was mostly done for CT195, as we succeeded in generating a CT195-deficient *C. trachomatis* strain. Overall, the mutant strain revealed that CT195, as IncM (Luís et al., 2023) and Dre1 (Sherry et al., 2022), contributes for the ability of *C. trachomatis* to induce multinucleation in infected cells. Furthermore, CT195 seems to inhibit *chlamydia* growth and fusion between inclusions, which has not been observed before for other chlamydial Incs and effectors.

Immunofluorescence microscopy to analyse the subcellular localization of CT195 and CT214 revealed not only that they both localize at the inclusion membrane, but also that CT214 localized at inclusion membrane microdomains (Mital et al., 2010). These microdomains have been observed near the centrosome and served as platforms for heterophilic interactions between Incs, as well as interactions with the centrosome, microtubules and the cytoskeleton (Mital et al., 2010). Until now, nine Incs have been shown to localize in inclusion membrane microdomains (MrcA, CT222, IPAM, CT224, CT228, IncB, IncC, IncM and CT850) (Weber et al., 2015; Lutter et al., 2013; Mital et al., 2010). In the case of IncM, its localization in microdomains was only seen during the early stage of the chlamydial infectious cycle and, usually, IncM-labelled microdomains do not localize near the centrosome (Luís et al., 2023). We observed that most CT214 microdomains found at early times of infection co-localized with IncM microdomains. Although distinct from IncM, CT214 often localized near the host cell centrosome, similar to what has been reported (but not quantified) for other Incs (Mital et al., 2010). One appealing hypothesis is that Incs at microdomains may interact with each other and collaborate in their functions. In previous studies, four Incs have been shown to co-localize at inclusion microdomains (Mital et al., 2010) but only two of them were shown to interact (Gauliard et al., 2015). We aimed to test if CT214 and IncM could interact by bacterial two-hybrid but control experiments using constructs that were used before to test homotypic IncA-IncA interactions were not successful (Gauliard et al., 2015). Because in the meantime we obtained a CT195-deficient *C. trachomatis* strain, within this work we opted to focus on characterizing these strains and the analysis of the possible CT214-IncM interaction was

not pursued. In future studies this could be analysed using a described co-infection model using two chlamydial strains each producing CT214 or IncM with different epitope tags (Han & Derré, 2017).

To further characterize Incs CT195 and CT214, we aimed to obtain the corresponding *C. trachomatis*-deficient strain mutants. This was successful for the *ct195* mutant strain but not for the *ct214* mutant. The inability to obtain the *ct214* mutant strain by the TargeTron method could be due to the complexity of retargeting the group II intron, which does not always succeed, and may require additional attempts. Alternatively, *ct214* might be essential to *Chlamydia* survival. In fact, studies have been shown that in *chxR* (encoding a transcriptional activator) null mutants, a set of genes, including *ct214*, was downregulated, and these mutants displayed significant growth deficiencies *in vivo*, though this was not observed it *in vitro* (Yang et al., 2017). This suggests that the expression of these genes, including *ct214*, might be crucial for *Chlamydia*. If we had succeeded in generating the *ct214* mutant, it would have been interesting to analyze its characteristics and investigate if it shared any functions with other Incs that localize in microdomains, especially with IncM due to their co-localization.

Obtaining the *ct195* mutant allowed us to start studying the role of CT195 in *C. trachomatis* infection of cultured cells. We begun by analyzing the mutant strain relative to its ability to grow intracellularly. We found that the presence of CT195 had a negative impact on chlamydial growth. To gain more insights in the reason why CT195 production would lead to this growth inhibition, we measured the inclusion area in cells infected by CT195-producing and -deficient strains. However, the absence of the protein did not have an effect in the inclusion area. As shown in previous studies, the size of the inclusion is not always a direct measure of chlamydial growth because the proteins produced by *Chlamydia* are the ones that dictate the expansion of the inclusion membrane, rather than bacterial replication itself (Engström et al., 2015). Therefore, CT195 does not appear to have a role in the expansion of inclusion. We also analyzed for a possible CT195-dependent defect in homotypic fusion between inclusions in the same host cell. This fusion between inclusions has been shown to depend on IncA (Hackstadt et al., 1999). Our experiments revealed that the presence of CT195 slightly delays the homotypic fusion between inclusions. We also analyzed whether CT195 could participate in chlamydial host cell exit, as it has been discovered that Incs like MrcA or CT228 regulate chlamydial release by extrusion (Nguyen et al., 2018; Lutter et al., 2013). Our experiments did not reveal a role of CT195 in chlamydial host cell exit. However, there was a significant variation between experiments suggesting that further studies are required for a solid conclusion on this topic.

Overall, the results described above suggest that CT195 regulates chlamydial growth, possibly to avoid the detection by the immune system or to help manage the resources available. However, this CT195-dependent reduction in chlamydial growth was observed in HeLa cells, which have limitations, including the lack of an accurate environment that recreates their tissue culture origin (Zhong et al., 2020), such as the presence of immune cells and other components of the immune system. Another possible explanation for the CT195-dependent reduction in chlamydial growth would be to maintain the integrity of the inclusion membrane. If this was the case, we should have detected an increase of

extracellular infectious chlamydiae in our assays of chlamydial host cell exit. However, also due to experimental variability in our assay, additional analyses of inclusion lysis should be required to clarify this point. It is intriguing that CT195 inhibits both chlamydial growth and homotypic fusion between inclusions, but at the moment it is unknown whether these two inhibitory activities of CT195 are linked. However, if the inhibition in chlamydial growth occurs from the beginning of the infection, and if the homotypic fusion between inclusions depends on bacterial replication, then this might explain the delayed fusion between inclusions as a consequence of the reduced chlamydial replication. Further research is required to determine how CT195 regulates the chlamydial growth and how this linked to its inhibitory activity on fusion between inclusions.

C. trachomatis infection can lead to host cell multinucleation by inhibiting the last step of cytokinesis, known as abscission (Brown et al., 2012; Greene, 2003; Sun et al., 2011). This has been proposed to be accomplished by chlamydial effectors that interact with host cell proteins involved in mitosis. While some studies suggest that cytokinesis inhibition is due to the strategic positioning of the inclusion within the host cell (Sun et al., 2011), others propose that the blockage is the result of a combined effect of *Chlamydia*-induced centrosome repositioning, centrosome amplification and early mitotic exit due to abnormal spindle formation (Sütterlin & Derré, 2020; Elwell et al., 2016). In contrast, other studies (Wang et al., 2021; Luís, 2024) argue that the centrosome amplification is a consequence of cytokinesis inhibition rather than a cause. It has also been reported that chlamydia induction of host cell multinucleation increases the contents of the Golgi apparatus facilitating the acquisition of lipids (Sun et al., 2015). Although the mechanisms by which Incs inhibit cytokinesis are still not fully understood, there has been a few possible explanations. For instance, we hypothesized that IncM may interact with or displace host cell proteins involved in the final steps of cell division or interfere with the microtubule network around the inclusion (Luís, 2024). In the case of Dre1, its induced mispositioning of the centrosome is suggested to cause abnormal spindle formation, which interferes with cytokinesis (Sherry et al., 2022). In a study based on the ectopic production by transient transfection of Incs IPAM, Tri1, and CT225 in mammalian cells it was found that they inhibit cytokinesis in these conditions (Alzhanov et al., 2009). The authors hypothesized that Incs affected host cell cycle control by disrupting the function of regulatory proteins (Alzhanov et al., 2009). In this work, we identified CT195 as another *C. trachomatis* protein that promotes multinucleation in infected cells possibly by interfering with host cell cytokinesis. However, our results showed that CT195 does not play a role in the ability of *C. trachomatis* to mediate centrosome mispositioning or to affect Golgi distribution around the inclusion. So, we can at least rule out the mispositioning of centrosomes as the cause for CT195 to lead to multinucleated host cells. In contrast to previous studies, although there were more multinucleated cells (Sherry et al., 2022; Luís et al., 2023), there were no CT195-dependent differences in Golgi distribution. This could mean that although the Golgi apparatus is increased in multinucleated cells, its recruitment and distribution around the inclusion is not influenced by the inhibition of cytokinesis or at least it is not related with CT195. Therefore, it is more likely that CT195 could promote the inhibition of cytokinesis by disrupting the normal function of host cell proteins involved in cytokinesis. Further investigation to

identify possible interactions with the host cell proteins that were observed to have its function altered in infected cells and to analyze if these *Chlamydia* effectors work together would provide insights into the mechanism used by *C. trachomatis* to inhibit host cell cytokinesis.

Considering that both CT195 and CT214 are proteins conserved in all biovars of *C. trachomatis* (Lutter et al., 2012) this supports that these proteins are important for infection. Further studies focusing on the interactions between Incs and host cell proteins or other Incs are highly required to better understand the mechanisms by which *C. trachomatis* manipulates all these host cell processes.

REFERENCES

Almeida, F., Luís, M. P., Pereira, I. S., Pais, S. V., & Mota, L. J. (2018). The Human Centrosomal Protein CCDC146 Binds *Chlamydia trachomatis* Inclusion Membrane Protein CT288 and Is Recruited to the Periphery of the *Chlamydia*-Containing Vacuole. *Frontiers in Cellular and Infection Microbiology*, *8*, 254. https://doi.org/10.3389/fcimb.2018.00254

Alzhanov, D. T., Weeks, S. K., Burnett, J. R., & Rockey, D. D. (2009). Cytokinesis is blocked in mammalian cells transfected with *Chlamydia trachomatis* gene *ct223*. *BMC Microbiology*, *9*. https://doi.org/10.1186/1471-2180-9-2

Battesti, A., & Bouveret, E. (2012). The bacterial two-hybrid system based on adenylate cyclase reconstitution in *Escherichia coli*. *Methods*, *58*(4), 325–334. https://doi.org/10.1016/j.ymeth.2012.07.018

Belland, R. J., Zhong, G., Crane, D. D., Hogan, D., Sturdevant, D., Sharma, J., Beatty, W. L., & Caldwell, H. D. (2003). Genomic transcriptional profiling of the developmental cycle of *Chlamydia trachomatis*. In *PNAS July* (Vol. 8, Issue 14). www.pnas.orgcgidoi10.1073pnas.1331135100

Bishop, R. C., & Derré, I. (2022). The *Chlamydia trachomatis* Inclusion Membrane Protein CTL0390 Mediates Host Cell Exit via Lysis through STING Activation. *Infection and Immunity*, *90*(6). https://doi.org/10.1128/iai.00190-22

Brown, H. M., Knowlton, A. E., & Grieshaber, S. S. (2012). Chlamydial infection induces host cytokinesis failure at abscission. *Cellular Microbiology*, *14*(10), 1554–1567. https://doi.org/10.1111/j.1462-5822.2012.01820.x

Brown, H. M., Knowlton, A. E., Snavely, E., Nguyen, B. D., Richards, T. S., & Grieshaber, S. S. (2014). Multinucleation during *C. trachomatis* Infections Is Caused by the Contribution of Two Effector Pathways. *PLoS ONE*, *9*(6), e100763. https://doi.org/10.1371/journal.pone.0100763

Bugalhão, J. N., & Mota, L. J. (2019). The multiple functions of the numerous *Chlamydia trachomatis* secreted proteins: the tip of the iceberg. *Microbial Cell*, *6*(9), 414–449. https://doi.org/10.15698/mic2019.09.691

Cingolani, G., McCauley, M., Lobley, A., Bryer, A. J., Wesolowski, J., Greco, D. L., Lokareddy, R. K., Ronzone, E., Perilla, J. R., & Paumet, F. (2019). Structural basis for the homotypic fusion of chlamydial inclusions by the SNARE-like protein IncA. *Nature Communications*, *10*(1). https://doi.org/10.1038/s41467-019-10806-9

da Cunha, M., Pais, S. V., Bugalhão, J. N., & Mota, L. J. (2017). The *Chlamydia trachomatis* type III secretion substrates CT142, CT143, and CT144 are secreted into the lumen of the inclusion. *PLOS ONE*, *12*(6), e0178856. https://doi.org/10.1371/journal.pone.0178856

Dautin, N., Karimova, G., Ullmann, A., & Ladant, D. (2000). Sensitive Genetic Screen for Protease Activity Based on a Cyclic AMP Signaling Cascade in *Escherichia coli. Journal of Bacteriology, 182*(24), 7060–7066. https://doi.org/10.1128/jb.182.24.7060-7066.2000

Dehoux, P., Flores, R., Dauga, C., Zhong, G., & Subtil, A. (2011). Multi-genome identification and characterization of *chlamydiae*-specific type III secretion substrates: the Inc proteins. *BMC Genomics*, *12*(1). https://doi.org/10.1186/1471-2164-12-109

Delevoye, C., Nilges, M., Dautry-Varsat, A., & Subtil, A. (2004). Conservation of the Biochemical Properties of IncA from *Chlamydia trachomatis* and *Chlamydia caviae*. *Journal of Biological Chemistry*, *279*(45), 46896–46906. https://doi.org/10.1074/jbc.m407227200

Derré, I., Swiss, R., & Agaisse, H. (2011). The lipid transfer protein CERT interacts with the Chlamydia inclusion protein IncD and participates to ER-*Chlamydia* inclusion membrane contact sites. *PLoS Pathogens*, *7*(6). https://doi.org/10.1371/journal.ppat.1002092

Dumoux, M., Menny, A., Delacour, D., & Hayward, R. D. (2015). A *Chlamydia* effector recruits CEP170 to reprogram host microtubule organization. *Journal of Cell Science*, *128*(18), 3420–3434. https://doi.org/10.1242/jcs.169318

Elwell, C. A., Czudnochowski, N., von Dollen, J., Johnson, J. R., Nakagawa, R., Mirrashidi, K., Krogan, N. J., Engel, J. N., & Rosenberg, O. S. (2017). *Chlamydia* interfere with an interaction between the mannose-6-phosphate receptor and sorting nexins to counteract host restriction. https://doi.org/10.7554/eLife.22709.001

Elwell, C., Mirrashidi, K., & Engel, J. (2016). *Chlamydia* cell biology and pathogenesis. *Nature Reviews Microbiology*, *14*(6), 385–400. https://doi.org/10.1038/nrmicro.2016.30

Engström, P., Bergström, M., Alfaro, A. C., Syam Krishnan, K., Bahnan, W., Almqvist, F., & Bergström, S. (2015). Expansion of the *Chlamydia trachomatis* inclusion does not require bacterial replication. https://doi.org/10.1016/j.ijmm.2015.02.007

European Centre for Disease Prevention and Control. (2017, November 20). *Facts about chlamydia*. European Centre for Disease Prevention and Control. https://www.ecdc.europa.eu/en/chlamydia/facts

Faris, R., Merling, M., Andersen, S. E., Dooley, C. A., Hackstadt, T., & Weber, M. M. (2019). *Chlamydia trachomatis* CT229 Subverts Rab GTPase-Dependent CCV Trafficking Pathways to Promote Chlamydial Infection. *Cell Reports*, *26*(12), 3380-3390.e5. https://doi.org/10.1016/j.celrep.2019.02.079

Gauliard, E., Ouellette, S. P., Rueden, K. J., & Ladant, D. (2015). Characterization of interactions between inclusion membrane proteins from *Chlamydia trachomatis*. *Frontiers in Cellular and Infection Microbiology*, *5*. https://doi.org/10.3389/fcimb.2015.00013

Greene, W. (2003). Inhibition of host cell cytokinesis by *Chlamydia trachomatis* infection. *Journal of Infection*, *47*(1), 45–51. https://doi.org/10.1016/s0163-4453(03)00039-2

Hackstadt, T., Scidmore-Carlson, M. A., Shaw, E. I., & Fischer, E. R. (1999). The *Chlamydia trachomatis* IncA protein is required for homotypic vesicle fusion. *Cellular Microbiology*, *1*(2), 119–130. https://doi.org/10.1046/j.1462-5822.1999.00012.x

Haines, A., Wesolowski, J., Ryan, N. M., Tiago Monteiro-Brás, & Fabienne Paumet. (2021). Cross Talk between ARF1 and RhoA Coordinates the Formation of Cytoskeletal Scaffolds during *Chlamydia* Infection. *MBio*, *12*(6). https://doi.org/10.1128/mbio.02397-21

Han, Y., & Derré, I. (2017). A Co-infection Model System and the Use of Chimeric Proteins to Study *Chlamydia* Inclusion Proteins Interaction. *Frontiers in Cellular and Infection Microbiology*, *7*. https://doi.org/10.3389/fcimb.2017.00079

Heuer, D., Lipinski, A. R., Machuy, N., Karlas, A., Wehrens, A., Siedler, F., Brinkmann, V., & Meyer, T. F. (2008). *Chlamydia* causes fragmentation of the Golgi compartment to ensure reproduction. *Nature*, *457*(7230), 731–735. https://doi.org/10.1038/nature07578

Kannan, R. M., Gérard, H. C., Mishra, M. K., Mao, G., Wang, S., Hali, M., Whittum-Hudson, J. A., & Hudson, A. P. (2013). Dendrimer-enabled transformation of *Chlamydia trachomatis*. *Microbial Pathogenesis*, *65*, 29–35. https://doi.org/10.1016/j.micpath.2013.08.003

Karimova, G., Pidoux, J., Ullmann, A., & Ladant, D. (1998). A bacterial two-hybrid system based on a reconstituted signal transduction pathway. *Proceedings of the National Academy of Sciences*, *95*(10), 5752–5756. https://doi.org/10.1073/pnas.95.10.5752

Key, C. E., & Fisher, D. J. (2016). Use of Group II Intron Technology for Targeted Mutagenesis in *Chlamydia trachomatis*. *Methods in Molecular Biology*, 163–177. https://doi.org/10.1007/978-1-4939-6472-7_11

Kokes, M., Dunn, J., Granek, Joshua A., Nguyen, Bidong D., Barker, Jeffrey R., Valdivia, Raphael H., & Bastidas, Robert J. (2015). Integrating Chemical Mutagenesis and Whole-Genome Sequencing as a Platform for Forward and Reverse Genetic Analysis of *Chlamydia*. *Cell Host & Microbe*, *17*(5), 716–725. https://doi.org/10.1016/j.chom.2015.03.014

Kozusnik, T., Adams, S. E., & Greub, G. (2024). Aberrant Bodies: An Alternative Metabolic Homeostasis Allowing Survivability? *Microorganisms*, *12*(3), 495. https://doi.org/10.3390/microorganisms12030495

Li, Z., Chen, C., Chen, D., Wu, Y., Zhong, Y., & Zhong, G. (2008). Characterization of Fifty Putative Inclusion Membrane Proteins Encoded in the *Chlamydia trachomatis* Genome. *Infection and Immunity*, *76*(6), 2746–2757. https://doi.org/10.1128/iai.00010-08

Luís, M. P. (2024). Manipulation of host cells by *Chlamydia trachomatis*: function and subcellular localization of an inclusion membrane protein. http://hdl.handle.net/10362/170186

Luís, M. P., Pereira, A. C., Soares, L. & Mota, L. J. (manuscript submitted for publication) The precise subcellular localization of *Chlamydia trachomatis* inclusion membrane proteins depends on the promoter used for their gene expression.

Luís, M. P., Pereira, I. S., Bugalhão, J. N., Simões, C. N., Mota, C., Romão, M. J., & Mota, L. J. (2023). The *Chlamydia trachomatis* IncM Protein Interferes with Host Cell Cytokinesis, Centrosome Positioning, and Golgi Distribution and Contributes to the Stability of the Pathogen-Containing Vacuole. *Infection and Immunity*, *91*(4). https://doi.org/10.1128/iai.00405-22

Lutter, E. I., Barger, A. C., Nair, V., & Hackstadt, T. (2013). *Chlamydia trachomatis* Inclusion Membrane Protein CT228 Recruits Elements of the Myosin Phosphatase Pathway to Regulate Release Mechanisms. *Cell Reports*, *3*(6), 1921–1931. https://doi.org/10.1016/j.celrep.2013.04.027

Lutter, E. I., Martens, C., & Hackstadt, T. (2012). Evolution and conservation of predicted inclusion membrane proteins in *chlamydiae*. *Comparative and Functional Genomics*, *2012*, 1–13. https://doi.org/10.1155/2012/362104

Manoj Kumar Mishra, Gérard, H. C., Whittum-Hudson, J. A., Hudson, A. P., & Kannan, R. M. (2012). Dendrimer-Enabled Modulation of Gene Expression *in Chlamydia trachomatis*. *Molecular Pharmaceutics*. https://doi.org/10.1021/mp200512f

Mital, J., Lutter, E. I., Barger, A. C., Dooley, C. A., & Hackstadt, T. (2015). *Chlamydia trachomatis* inclusion membrane protein CT850 interacts with the dynein light chain DYNLT1 (Tctex1). *Biochemical and Biophysical Research Communications*, *462*(2), 165–170. https://doi.org/10.1016/j.bbrc.2015.04.116

Mital, J., Miller, N. J., Fischer, E. R., & Hackstadt, T. (2010). Specific chlamydial inclusion membrane proteins associate with active Src family kinases in microdomains that interact with the host microtubule network. *Cellular Microbiology*, *12*(9), 1235–1249. https://doi.org/10.1111/j.1462-5822.2010.01465.x

Mohseni, M., Sung, S., & Takov, V. (2023, August 8). *Chlamydia*. Nih.gov; StatPearls Publishing. https://www.ncbi.nlm.nih.gov/books/NBK537286/#article-19431.s20

Nguyen, P. H., Lutter, E. I., & Hackstadt, T. (2018). *Chlamydia trachomatis* inclusion membrane protein MrcA interacts with the inositol 1,4,5-trisphosphate receptor type 3 (ITPR3) to regulate extrusion formation. *PLoS Pathogens*, *14*(3). https://doi.org/10.1371/journal.ppat.1006911

Nunes, A., & Gomes, J. P. (2014). Evolution, phylogeny, and molecular epidemiology of *Chlamydia*. *Infection, Genetics and Evolution: Journal of Molecular Epidemiology and Evolutionary Genetics in Infectious Diseases*, *23*, 49–64. https://doi.org/10.1016/j.meegid.2014.01.029

O'Neill, C. E., Clarke, I. N., & Fisher, D. J. (2020). *Chlamydia* Genetics. *Caister Academic Press EBooks*. https://doi.org/10.21775/9781912530281.11

Olson, M. G., Goldammer, M., Gauliard, E., Ladant, D., & Ouellette, S. P. (2018). A Bacterial Adenylate Cyclase-Based Two-Hybrid System Compatible with Gateway® Cloning. *Methods in Molecular Biology (Clifton, N.J.)*, *1794*, 75–96. https://doi.org/10.1007/978-1-4939-7871-7_6

Panzetta, M. E., Valdivia, R. H., & Saka, H. A. (2018). *Chlamydia* Persistence: A Survival Strategy to Evade Antimicrobial Effects in-vitro and in-vivo. *Frontiers in Microbiology*, *9*. https://doi.org/10.3389/fmicb.2018.03101

Ronzone, E., & Paumet, F. (2013). Two Coiled-Coil Domains of *Chlamydia trachomatis* IncA Affect Membrane Fusion Events during Infection. *PLoS ONE*, *8*(7). https://doi.org/10.1371/journal.pone.0069769

Schindelin, J., Arganda-Carreras, I., Frise, E., Kaynig, V., Longair, M., Pietzsch, T., Preibisch, S., Rueden, C., Saalfeld, S., Schmid, B., Tinevez, J.-Y., White, D. J., Hartenstein, V., Eliceiri, K., Tomancak, P., & Cardona, A. (2012). Fiji: an open-source Platform for biological-image Analysis. *Nature Methods*, *9*(7), 676–682. https://doi.org/10.1038/nmeth.2019

Scidmore, M. A. (2005). Cultivation and Laboratory Maintenance of *Chlamydia trachomatis*. *Current Protocols in Microbiology*, *Chapter 11*, Unit 11A.1. https://doi.org/10.1002/9780471729259.mc11a01s00

Shaw, E. I., Dooley, C. A., Fischer, E. R., Scidmore, M. A., Fields, K. A., & Hackstadt, T. (2000). Three temporal classes of gene expression during the *Chlamydia trachomatis* developmental cycle. *Molecular Microbiology*, *37*(4), 913–925. https://doi.org/10.1046/j.1365-2958.2000.02057.x

Sherry, J., Dolat, L., MacMahon, E., Swaney, D. L., Bastidas, R. J., Johnson, J. R., Valdivia, R. H., Krogan, N. J., Elwell, C. A., & Engel, J. N. (2022). *Chlamydia trachomatis* effector Dre1 interacts with dynactin to reposition host organelles during infection. *BioRxiv (Cold Spring Harbor Laboratory)*. https://doi.org/10.1101/2022.04.15.488217

Sixt, B. S., Bastidas, R. J., Finethy, R., Baxter, R. M., Carpenter, V. K., Kroemer, G., Coers, J., & Valdivia, R. H. (2017). The *Chlamydia trachomatis* Inclusion Membrane Protein CpoS Counteracts STING-Mediated Cellular Surveillance and Suicide Programs. *Cell Host and Microbe*, *21*(1), 113–121. https://doi.org/10.1016/j.chom.2016.12.002

Stanhope, R., Flora, E., Bayne, C., & Derré, I. (2017). IncV, a FFAT motif-containing *Chlamydia* protein, tethers the endoplasmic reticulum to the pathogen-containing vacuole. *Proceedings of the National Academy of Sciences of the United States of America*, *114*(45), 12039–12044. https://doi.org/10.1073/pnas.1709060114

Stephens, R. S., Kalman, S., Lammel, C., Fan, J., Marathe, R., Aravind, L., Mitchell, W., Olinger, L., Tatusov, R. L., Zhao, Q., Koonin, E. V., & Davis, R. W. (1998). Genome sequence of an obligate intracellular pathogen of humans: *Chlamydia trachomatis*. *Science (New York, N.Y.)*, *282*(5389), 754–759. https://doi.org/10.1126/science.282.5389.754

Sun, H. S., Sin, A. T., Poirier, M. B., & Harrison, R. E. (2015). *Chlamydia trachomatis* Inclusion Disrupts Host Cell Cytokinesis to Enhance Its Growth in Multinuclear Cells. *Journal of Cellular Biochemistry*, *117*(1), 132–143. https://doi.org/10.1002/jcb.25258

Sun, H. S., Wilde, A., & Harrison, R. E. (2011). *Chlamydia trachomatis* Inclusions Induce Asymmetric Cleavage Furrow Formation and Ingression Failure in Host Cells. *Molecular and Cellular Biology*, *31*(24), 5011–5022. https://doi.org/10.1128/mcb.05734-11

Sütterlin, C., & Derré, I. (2020). Interactions of the Chlamydial Inclusion with the Host Cell. In *Chlamydia Biology From Genome to Disease* (pp. 111–134). Caister Academic Press eBooks. https://doi.org/10.21775/9781912530281.05

Tam, J. E., Davis, C. H., & Wyrick, P. B. (1994). Expression of recombinant DNA introduced into *Chlamydia trachomatis* by electroporation. *Canadian Journal of Microbiology*, *40*(7), 583–591. https://doi.org/10.1139/m94-093

Verbeke, P., Welter-Stahl, L., Ying, S., Hansen, J., Häcker, G., Darville, T., & Ojcius, D. M. (2006). Recruitment of BAD by the *Chlamydia trachomatis* vacuole correlates with host-cell survival. *PLoS Pathogens*, *2*(5), 408–417. https://doi.org/10.1371/journal.ppat.0020045

Walsh, S. C., Reitano, J. R., Dickinson, M. S., Kutsch, M., Hernandez, D., Barnes, A. B., Schott, B. H., Wang, L., Ko, D. C., Kim, S. Y., Valdivia, R. H., Bastidas, R. J., & Coers, J. (2022). The bacterial effector GarD shields *Chlamydia trachomatis* inclusions from RNF213-mediated ubiquitylation and destruction. *Cell Host and Microbe*, *30*(12), 1671-1684.e9. https://doi.org/10.1016/j.chom.2022.08.008

Wan, W., Li, D., Li, D., & Jiao, J. (2023). Advances in genetic manipulation of *Chlamydia trachomatis*. *Frontiers in Immunology*, *14*. https://doi.org/10.3389/fimmu.2023.1209879

Wang, K., Muñoz, K. J., Tan, M., & Sütterlin, C. (2021). *Chlamydia* and HPV induce centrosome amplification in the host cell through additive mechanisms. *Cellular Microbiology*, *23*(12). https://doi.org/10.1111/cmi.13397

Wang, X., Wu, H., Fang, C., & Li, Z. (2024). Insights into innate immune cell evasion by *Chlamydia trachomatis*. In *Frontiers in Immunology* (Vol. 15). Frontiers Media SA. https://doi.org/10.3389/fimmu.2024.1289644

Wang, Y., Kahane, S., Cutcliffe, L. T., Skilton, R. J., Lambden, P. R., & Clarke, I. N. (2011). Development of a transformation system for *Chlamydia trachomatis*: restoration of glycogen biosynthesis by acquisition of a plasmid shuttle vector. *PLoS Pathogens*, *7*(9), e1002258. https://doi.org/10.1371/journal.ppat.1002258

Weber, M. M., Bauler, L. D., Lam, J., & Hackstadt, T. (2015). Expression and Localization of Predicted Inclusion Membrane Proteins in *Chlamydia trachomatis*. *Infection and Immunity*, *83*(12), 4710–4718. https://doi.org/10.1128/iai.01075-15

Weber, M. M., Lam, J. L., Dooley, C. A., Noriea, N. F., Hansen, B. T., Hoyt, F. H., Carmody, A. B., Sturdevant, G. L., & Hackstadt, T. (2017). Absence of Specific *Chlamydia trachomatis* Inclusion Membrane Proteins

Triggers Premature Inclusion Membrane Lysis and Host Cell Death. *Cell Reports*, *19*(7), 1406–1417. https://doi.org/10.1016/j.celrep.2017.04.058

Wenbo, L., Yewei, Y., Hui, Z., & Zhongyu, L. (2024). Hijacking host cell vesicular transport: New insights into the nutrient acquisition mechanism of *Chlamydia*. In *Virulence* (Vol. 15, Issue 1). Taylor and Francis Ltd. https://doi.org/10.1080/21505594.2024.2351234

Wesolowski, J., Weber, M. M., Nawrotek, A., Dooley, C. A., Calderon, M., St Croix, C. M., Hackstadt, T., Cherfils, J., & Paumet, F. (2017). *Chlamydia* Hijacks ARF GTPases To Coordinate Microtubule Posttranslational Modifications and Golgi Complex Positioning. https://doi.org/10.1128/mBio

World Health Organization. (2023, July 17). *Chlamydia*. Www.who.int. https://www.who.int/news-room/fact-sheets/detail/chlamydia

Yang, C., Kari, L., Sturdevant, G. L., Song, L., Patton, M. J., Couch, C. E., Ilgenfritz, J. M., Southern, T. R., Whitmire, W. M., Briones, M., Bonner, C., Grant, C., Hu, P., McClarty, G., & Caldwell, H. D. (2017). *Chlamydia trachomatis* ChxR is a transcriptional regulator of virulence factors that function in in vivo host–pathogen interactions. *Pathogens and Disease*, *75*(3). https://doi.org/10.1093/femspd/ftx035

Zhong, G., Quayle, A., Aiyar, A., & Zhang, T. (2020). Animal Models of *Chlamydia trachomatis* Infection. In *Chlamydia Biology From Genome to Disease* (pp. 459–482). Caister Academic Press. https://doi.org/10.21775/9781912530281.19

Zhu, H., Shen, Z., Luo, H., Zhang, W., & Zhu, X. (2016). *Chlamydia Trachomatis* Infection-Associated Risk of Cervical Cancer. *Medicine*, *95*(13), e3077. https://doi.org/10.1097/md.0000000000003077

A

ANNEXES

Table A. 1. *Escherichia coli* strains used in this work.

Strain	Characteristics	Reference
E. coli NEB® 10β	DH10BTM derivative. Genotype: *Δ(ara-leu) 7697, araD139, fhuA, ΔlacX74, galK16, galE15 e14-, Φ80dlacZΔM15, recA1, relA1, endA1, nupG, rpsL (Str^R), rph, spoT1, Δ(mrr-hsdRMS-mcrBC).*	New England Biolabs
E. coli ER2925	Competent cells with a methyltransferase deficiency (lack of Dam and Dcm methylation) Genotype: *ara-14, leuB6, fhuA31, lacY1, tsx78, glnV44, galK2, galT22, mcrA, dcm-6, hisG4, rfbD1, R(zgb210::Tn10), TetS, endA1, rpsL136, dam13::Tn9, xylA-5, mtl-1, thi-1, mcrB1, hsdR2.*	New England Biolabs
E. coli BTH101	*cya* mutant strain that relies on adenylate cyclase activity for *lac* operon activation and it is used in the BACTH system to detect protein-protein interactions. Genotype: *F', cya-99, araD139, galE15, galK16, rpsL1 (Str^^R), hsdR2, mcrA1, mcrB1, relA1*	Dautin et al., 2000

Table A. 2. *Chlamydia trachomatis* strains used in this work.

Strain	Characteristics	Reference
L2/434/Bu ACE051	Wild-type strain (originally from Tony Maurelli's lab; University of Florida).	From Derek J. Fisher.
ct195::aadA	*C. trachomatis* L2/434/Bu derivative. The *ct195* gene was disrupted between nucleotides 160 and 161 by the insertion of a group II intron and a gene (*aadA*) that confers resistance to spectinomycin.	This work.
ct195::aadA (pML39)	*C. trachomatis ct195::aadA* strain harboring the pML39 plasmid which encodes for CT195 with a double hemagglutinin tag (CT195-2HA).	This work.
L2/434 (pML39)	*C. trachomatis* L2/434/Bu strain harboring the pML39 plasmid which encodes for CT195 with a double hemagglutinin tag (CT195-2HA).	This work.
L2/434 (pML33)	*C. trachomatis* L2/434/Bu strain harboring the pML33 plasmid which encodes for CT214 with a double hemagglutinin tag (CT214-2HA).	This work.

Table A. 3. Plasmids used in this work.

Plasmid	Description/Construction	Reference
pDFTT3aadA	Group II intron donor plasmid	Key and Fisher, 2016
pSVP247	Derivative of *C. trachomatis-E. coli* shuttle vector (p2TK2-SW2) for production of proteins with a C-terminal double hemagglutinin (2HA) tag. Contains the terminator of the *incDEFG* operon of *C. trachomatis* L2/434 (Amp^R).	da Cunha et al., 2017
pML39/pCT195-2HA	Derivative of pSVP247. Enables the production of CT195-2HA under the control of its native promoter (P*ct195*, 250 nucleotides upstream from the predicted starting codon). A DNA fragment comprising P*ct195*-*ct195* was amplified from *C. trachomatis* L2/434 chromosomal DNA using primers #2897 and #2898. The resulting DNA product was digested with KpnI and NotI and ligated into those sites of pSVP247 (Amp^R).	From Maria P. Luís
pML33/pCT214-2HA	Derivative of pSVP247. Enables the production of CT214-2HA under the control of its native promoter (P*ct214*, 250 nucleotides upstream from the predicted starting codon). A DNA fragment comprising P*ct214*-*ct214* was amplified from *C. trachomatis* L2/434 chromosomal DNA using primers #2867 and #2868. The resulting DNA product was digested with KpnI and NotI and ligated into those sites of pSVP247 (Amp^R).	From Maria P. Luís
pAB1	Derivative of pDFTT3aadA containing the *ctl0447/ct195* intron targeting sequence from *C. trachomatis* strain L2/434 (orthologue of *ct195* in strain D/UW3). To obtain this, the 5' intron sequence was amplified by PCR using primers #2921, #2925, #2922, and #1922. The resulting ~350 bp DNA product was digested with HindIII and BsrG1/Bsp1407I and ligated into those sites of pDFTT3aadA.	This work
pAB2	Derivative of pDFTT3aadA containing the *ctl0466/ct214* intron targeting sequence from *C. trachomatis* strain L2/434 (orthologue of *ct214* in strain D/UW3). To obtain this, the 5' intron sequence was amplified by PCR using primers #2923, #2928, #2924, and #1922. The resulting ~350 bp DNA product was digested with HindIII and BsrG1/Bsp1407I and ligated into those sites of pDFTT3aadA.	This work

pKT25.zip	Positive control to BACTH assay: encodes N-terminal T25 cyclase fragment fused to a leucine zipper.	Olson et al., 2018
pUT18.zip	Positive control to BACTH assay: encodes C-terminal T18 cyclase fragment fused to a leucine zipper.	Olson et al., 2018
pUT18C	Encodes C-terminal T18 cyclase fragment.	Olson et al., 2018
pKT25	Encodes N-terminal T25 cyclase fragment.	Olson et al., 2018
His-pKT25	Derivative of pKT25. Encodes N-terminal T25 cyclase fragment fused to a His-tag in its upstream.	From Isabel Sá Nogueira laboratory; constructed by Joana Almeida.
pAB3	His-T25-IncA; derivative of His-pKT25. Encodes N-terminal T25 cyclase fragment fused to a His-tag at its N-terminus and IncA full length at its C-terminus. The incA gene was amplified from L2/434 chromosomal DNA using primers #2948 and #2949, digested with BamHI and KpnI and ligated into those sites of His-pKT25.	This work
pAB4	T18C-IncA-2HA; derivative of pUT18C. Encodes C-terminal T18 cyclase fragment fused to IncA full length with a C-terminal 2HA tag. The *incA* gene was amplified from L2/434 chromosomal DNA using primers using #2948 and #2954, digested with BamHI and KpnI and ligated into those sites of pUT18C.	This work

Table A. 4. Primers used in this work.

Code	Description	Sequence (5'->3')	Restriction enzyme
162	His-pKT25 sequencing (Fw)	TTCGCCATTATGCCGCATC	-
163	His-pKT25 sequencing (Rv)	TGCTGCAAGGCGATTAAG	-
164	pUT18C sequencing (Rv)	GGATGTACTGGAAACGGTG	-
165	pUT18C sequencing (Rv)	AACTATGCGGCATCAGAGC	-
1478	p2TK2-SW2 sequencing (Fw)	ATGGAAAAACGCCAGCAACG	-
1479	p2TK2-SW2 sequencing (Rv)	ACAAAATCAAAACAGAATCG	-
1864	Complementary to group II intron; PCR verification of strain *ct195::aadA* (Fw)	AGCGATGCCGAGAATCTG	-
1865	Complementary to group II intron; PCR verification of strain *ct195::aadA* (Rv)	TCTCGGAGTATACGGCTCTG	-
1922	Group II intron retargeting (EBS universal)	CGAAATTAGAAACTTGCGTTCAGTAAAC	-
2867	Generation of pML33 and PCR verification of *C. trachomatis* L2/434 (pML33) strain (Fw)	GATCGGTACCTCTCCGTCAGAGCGGATGC	KpnI
2868	Generation of pML33 and PCR verification of *C. trachomatis* L2/434 (pML33) strain (Rv)	GATCGCGGCCGCAACCAAATAATGCAGGTAGAGC	NotI
2897	Generation of pML39 and PCR verification of *C. trachomatis* L2/434 (pML39), *ct195::aadA,* and *ct195::aadA* (pML39) strains (Fw)	GATCGGTACCAATTAGGATTAACTGTTGTTGC	KpnI
2898	Generation of pML39 and PCR verification of *C. trachomatis* L2/434 (pML39) and *ct195::aadA* strains (Rv)	GATCGCGGCCGCAAAAGCTGGCCAACCTTCCTG	NotI
2921	Group II intron retargeting (195_160|161s_IBS1/2); locus-specific DNA sequencing of strain *ct195::aadA*	AAAAAAGCTTATAATTATCCTTACGGCTCGTGTTAGTGCGCCCAGATAGGGTG	HindIII
2922	Group II intron retargeting (195_160|161s_EBS2); locus-specific DNA sequencing of strain *ct195::aadA*.	TGAACGCAAGTTTCTAATTTCGATTAGCCGTCGATAGAGGAAAGTGTCT	-

2923	Group II intron retargeting (214_301|302s_IBS1/2); locus-specific DNA sequencing of strain *ct214::aadA.*	AAAAAAGCTTATAATTATCC TTAGACCACTACTCAGTGC GCCCAGATAGGGTG	HindIII
2924	Group II intron retargeting (214_301|302s_EBS2); locus-specific DNA sequencing of strain *ct214::aadA.*	TGAACGCAAGTTTCTAATTT CGATTTGGTCTCGATAGAG GAAAGTGTCT	-
2925	Group II intron retargeting (195_160|161s_EBS1/d); locus-specific DNA sequencing of strain *ct195::aadA.*	CAGATTGTACAAATGTGGTG ATAACAGATAAGTCGTGTTA TTTAACTTACCTTTCTTTGT	BsrG1/ Bsp1407I
2928	Group II intron retargeting (214_301|302s_EBS1/d); locus-specific DNA sequencing of strain *ct214::aadA.*	CAGATTGTACAAATGTGGTG ATAACAGATAAGTCTACTCA AGTAACTTACCTTTCTTTGT	BsrG1/ Bsp1407I
2947	pAB4 construction: amplification of *incA* (Rv).	GATCGGTACCCTAAGCATA ATCAGGAACATCATACGGAT ACGCATAGTCCGGCACATC ATACGGATAGGAGCTTTTTG TAGAGGGTG	KpnI
2948	pAB3 and pAB4 construction: amplification of *incA* (Fw).	GATCGGATCCCACAACGCC TACTCTAATCG	BamHI
2949	pAB3 construction: amplification of *incA* (Rv).	GATCGGTACCCTAGGAGCT TTTTGTAGAGGG	KpnI
2954	PCR verification of *C. trachomatis* ct195::aadA (pML39) strain (Rv)	GATCGGTACCCTAAGCATA ATCAGGAACATCATACG	-